Brain, Behavior, and Immunity 117 (2024) 51–65

Contents lists available at ScienceDirect

Brain Behavior and Immunity

journal homepage: www.elsevier.com/locate/ybrbi

Full-length Article

Microglial STING activation alleviates nerve injury-induced neuropathic pain in male but not female mice

Arthur Silveira Prudente [a,1], Sang Hoon Lee [a,1], Jueun Roh [a,b], Debora D. Luckemeyer [a], Cinder F. Cohen [a], Marie Pertin [c,d], Chul-Kyu Park [b], Marc R. Suter [c,d], Isabelle Decosterd [c,d], Jun-Ming Zhang [a], Ru-Rong Ji [e,f], Temugin Berta [a,*]

[a] Pain Research Center, Department of Anesthesiology, University of Cincinnati Medical Center, Cincinnati, OH, USA
[b] Department of Physiology, Gachon Pain Center, Gachon University College of Medicine, Incheon, South Korea
[c] Pain Center, Department of Anesthesiology, Lausanne University Hospital (CHUV) and University of Lausanne, 1011 Lausanne, Switzerland
[d] Department of Fundamental Neurosciences, Faculty of Biology and Medicine, University of Lausanne, 1011 Lausanne, Switzerland
[e] Center for Translational Pain Medicine, Department of Anesthesiology, Duke University Medical Center, Durham, NC, USA
[f] Departments of Cell Biology and Neurobiology, Duke University Medical Center, Durham, NC, USA

ARTICLE INFO

Keywords:
Neuropathic pain
Microglia
STING
Spared nerve injury
Sex difference
Interferon
Cytokines

ABSTRACT

Microglia, resident immune cells in the central nervous system, play a role in neuroinflammation and the development of neuropathic pain. We found that the stimulator of interferon genes (STING) is predominantly expressed in spinal microglia and upregulated after peripheral nerve injury. However, mechanical allodynia, as a marker of neuropathic pain following peripheral nerve injury, did not require microglial STING expression. In contrast, STING activation by specific agonists (ADU-S100, 35 nmol) significantly alleviated neuropathic pain in male mice, but not female mice. STING activation in female mice leads to increase in proinflammatory cytokines that may counteract the analgesic effect of ADU-S100. Microglial STING expression and type I interferon-ß (IFN-ß) signaling were required for the analgesic effects of STING agonists in male mice. Mechanistically, downstream activation of TANK-binding kinase 1 (TBK1) and the production of IFN-ß, may partly account for the analgesic effect observed. These findings suggest that STING activation in spinal microglia could be a potential therapeutic intervention for neuropathic pain, particularly in males.

1. Introduction

Peripheral nerve injury can cause neuropathic pain, including mechanical allodynia, which is a major concern in patients (Jensen and Finnerup, 2014). Neuropathic pain is resistant to current analgesics, which often target neuronal pathways and come with adverse effects (Grosser et al., 2017; Ji et al., 2014). Microglia are resident immune cells in the central nervous system (CNS) that constantly monitor their environment and mount neuroinflammatory responses, which underlie neurological diseases (Li and Barres, 2018). Evidence suggests that spinal microglia and neuroinflammation play a role in the development and maintenance of neuropathic pain, making them a potential target for therapeutic intervention (Ji et al., 2013). However, treatments targeting microglial and neuroinflammatory mechanisms had disappointing results in patients with neuropathic pain (Eisenach et al., 2010; Ostenfeld et al., 2015; Vanelderen et al., 2015; Younger and Mackey, 2009). These results may be due to a lack of biomarkers, non-specific effects of agents studied, lack of understanding of sex dimorphism and distinct contributions of microglial signaling pathways (Chen et al., 2018), some of which may indeed promote the resolution of neuropathic pain (Kohno et al., 2022).

The stimulator of interferon genes (STING, also known as TMEM173) is a pattern recognition receptor (PRR) for the cytosolic DNA-sensing pathway, which was originally discovered as a mediator of immune responses against pathogens (Ishikawa and Barber, 2008). The STING pathway is typically triggered when the sensor cyclic-GMP-AMP synthase (cGAS) detects cytosolic DNA (Burdette and Vance, 2013), which leads to the recruitment of TANK-binding kinase 1 (TBK1) and the

* Corresponding author at: Pain Research Center, Department of Anesthesiology, University of Cincinnati College of Medicine, 231 Albert Sabin Way, ML 0531, Cincinnati, OH 45267-0531, USA.
E-mail address: temugin.berta@uc.edu (T. Berta).
[1] First co-authors.

https://doi.org/10.1016/j.bbi.2024.01.003
Received 21 September 2023; Received in revised form 21 December 2023; Accepted 3 January 2024
Available online 6 January 2024

phosphorylation of the transcription factor interferon regulatory factor 3 (IRF3). IRF3 is then transported to the nucleus and initiates the transcription of type I interferons (IFN-Is) and proinflammatory cytokines (Barber, 2014). To note, the STING pathway also triggers proinflammatory cytokines through the activity of nuclear factor-κB (NF-κB) (Balka et al., 2020; Ishikawa and Barber, 2008). Studies of the STING pathway have mostly been conducted in infectious diseases and cancer (Fritsch et al., 2023). New research suggests that, although it is still in its infancy, STING may also be important in neuroinflammatory and neurological diseases, such as neuropathic pain (Chin, 2019; Tan et al., 2021; Yang et al., 2022).

Our recent study reported that STING is expressed in sensory neurons of the dorsal root ganglia (DRGs) and intrathecal injections of STING agonists can inhibit nociception through IFN-I signaling (Donnelly et al., 2021). Surprisingly, intrathecal injections of a STING antagonist (C-176) also alleviate neuropathic pain, possibly by targeting STING expression in spinal microglia and controlling neuroinflammation (Sun et al., 2022; Wu et al., 2022). Because these studies suggest that STING is expressed in various cell types and intrathecal route can target both DRG and spinal tissues, its overall role in controlling nociception, neuroinflammation, and neuropathic pain is still unclear. Since STING is highly expressed in microglia (Donnelly et al., 2021; Gulen et al., 2023; Mathur et al., 2017), we hypothesized that gaining a better understanding of and modulating STING in these cells could lead to new treatments for neuropathic pain. This is especially relevant given that numerous drugs targeting STING in clinical trials for cancer patients (Kong et al., 2023), repurposing them for neuropathic pain treatment is worth considering.

In this study, we showed that in the spinal cord STING is predominantly, but not exclusively, expressed in microglia and its expression levels increase after peripheral nerve injury. Surprisingly, we demonstrated that the development of mechanical allodynia following peripheral nerve injury is independent of this microglial STING upregulation, by using a conditional mouse line lacking STING in microglia. However, we found that microglial STING expression and IFN-I signaling are required for the alleviation of neuropathic pain in male mice following intrathecal injections of STING agonists, but not in female mice.

2. Materials and methods

2.1. Animals

Adult CD1 mice (Stock No: 22, males and females, 8–12 weeks) were used for pharmacological and biochemical studies, and purchased from Charles River Laboratories. C57BL/6J control mice (Stock No: 000664), STING floxed/conditional knockout mice ($STING^{fx/fx}$, Stock No: 031670), Ai14 floxed/conditional reporter mice (Stock No: 007914), Tmem119-CreERT2 inducible mice (Stock No: 031820) were purchased from the Jackson Laboratory and transgenic mice maintained on a C57BL/6J background. Pirt-Cre mice, which were also maintained on a C57BL/6J background, were gifted to us by Xinzhong Dong from Johns Hopkins University. Mice were housed four per cage at 22 ± 0.5 °C under a controlled 14/10 h light/dark cycle, with food and water available ad libitum. All experimental procedures were approved by the Institutional Animal Care and Use Committee at the University of Cincinnati, in accordance with the National Institute of Health Guide for the Care and Use of Laboratory Animals. All results are reported according to Animal Research: reporting of in vivo Experiments (ARRIVE) guidelines (Percie Du Sert et al., 2020). Animals were assigned randomly to different experimental groups. Sample size were determined based on our previous similar studies (Berta et al., 2017; Liu et al., 2019; Tonello et al., 2020). Investigators were blind to animal treatments, no adverse effects were observed during these studies, and all animals were included in statistical analyses.

2.2. Drugs and intrathecal delivery

The following drugs were used in this study: ADU-S100 (Chemietek, Cat. No: CT-ADUS100), DMXAA (Cayman Chemical, Cat. No: 14617), GSK8612 (Selleckchem, Cat. No: S8872), anti-rat IFN-ß neutralizing antibody (PBL Assay Science, Cat. No: 224001), rat IgGs (R&D Systems, respectively Cat. No: AB1008C and 6001F). Some drugs were injected intrathecally by a spinal puncture was made with a 30-gauge needle between the L5 and L6 level, as previously described (Berta et al., 2014; Lee et al., 2018; Tonello et al., 2020).

2.3. Animal models of neuropathic pain

Neuropathic pain was produced using two common animal models: the spared nerve injury (SNI) and the chronic constriction injury (CCI) mouse models (Bennett and Xie, 1988; Decosterd and Woolf, 2000). For both models, mice were anaesthetized with isoflurane and the left leg was shaved, disinfected with 10 % povidone–iodine, and a 1 cm superficial incision was made to expose the sciatic nerve. For the SNI model, the common peroneal and tibial nerves were ligated with 6.0 silk suture (AD Surgical, Cat. No: SS618R13) and transected, and a 1–2 mm portion of the nerves was removed. For the CCI model, three ligatures (6–0 chromic gut suture, AD Surgical, Cat. No: PSC618R13) were placed around the nerve proximal to the trifurcation with a distance of 1 mm between each ligature. The ligatures were loosely tied until a short flick of the ipsilateral hind limb was observed. Animals in the sham groups received surgery identical to those described above but without nerve ligation or transection.

2.4. Behavior tests

von Frey filament assay - Mechanical sensitivity and development of allodynia as a readout for neuropathic pain were assessed as the hind paw withdrawal response to von Frey hair stimulations using the up-and-down method, as previously described (Chaplan et al., 1994). Briefly, the mice were first acclimatized (1 h) in individual clear Plexiglas boxes on an elevated wire mesh platform to facilitate access to the plantar surface of the hind paws. Subsequently, a series of von Frey hairs (0.02, 0.07, 0.16, 0.4, 0.6, 1.0, and 1.4 g; Stoelting CO., Wood Dale, IL) were applied perpendicular to the plantar surface of hind paw. A test began with the application of the 0.6 g hair. A positive response was defined as a clear paw withdrawal or shaking. Whenever a positive response occurred, the next lower hair was applied, and whenever a negative response occurred, the next higher hair was applied. The testing consisted of six stimuli, and the pattern of response was converted to a 50 % von Frey threshold, using the method described previously (Dixon, 1980).

Dry ice assay - Cold sensitivity was assessed in mice acclimated to the Plantar Test apparatus (IITC Life Science) for 20 min before cold stimulation with dry ice, according to a previously described protocol (Brenner et al., 2012). Briefly, a 10 ml syringe, sectioned above the Leur lock and tightly packed with finely crushed dry ice, was pressed firmly on the bottom of the tempered glass directly below the hindpaw. The paw withdrawal latency of the mice was measured with a stopwatch. A standard baseline and a cut off of 20 s were observed in naïve mice. All mice were tested three times, with at least 5 min between recordings. The average of all recordings was used for statistical analysis.

Pinprick assay – Nociceptive sensitivity was assessed using a slightly modified pinprick test previously described (Tochitsky et al., 2021). The animals were first placed in a square Plexiglas chamber on top of a wire

mesh table. Before conducting the test, the animals were acclimated in the arena for 1 h the day before and for an additional 30 min immediately before testing. A needle (27 G, BD Biosciences), along with a 1 g von Frey filament, was applied to the left hind paw with minimal pressure (0.96 g). The needle had a non-sharp tip to prevent skin penetration. The pinprick stimulus was applied five times, and the response rate was calculated.

Hargreaves assay - Heat sensitivity was measured in mice using the Plantar Test apparatus (IITC Life Science) and assessing paw withdrawal latency in response to heat stimulation, according to the Hargreaves method (Hargreaves et al., 1988). Animals were first acclimated in plastic observation boxes for 20 min. Then, the mid-plantar surface of the mouse hindpaw was exposed to a radiant heat source through a glass floor until paw withdrawal. The intensity of the heat was adjusted to produce a baseline of about 15 s in naïve mice, with a maximum cutoff of 20 s. Each mouse was tested three times, with at least two minutes between recordings. The average of all recordings was used for statistical analysis.

Rotarod assay (motor performance) - Motor performance was assessed using a Rotarod Treadmill from IITC Life Science. Mice received two consecutive days of training before testing. The latency to fall was measured with an accelerated rotation speed from 5 to 35 rpm over 3 min. All mice were tested three times with at least 10 min between recordings and the average of all recordings was used for statistical analysis.

2.5. In situ hybridization (i.e. RNAscope)

Mice were deeply anaesthetized with isoflurane and transcardially perfused with PBS followed by 4 % paraformaldehyde (PAF). Lumbar DRG and spinal cord tissues were isolated and post-fixed in PAF for 1–2 h before incubation overnight in a 30 % sucrose solution. Tissues were then embedded in OCT medium (Tissue-Tek) and cryosectioned at a thickness of 14–20 μm. RNAscope was performed following the manufacturer's instructions using the RNAscope Multiplex Fluorescent Reagent Kit v2 (Advanced Cell Diagnostics, Cat. No: 323110). Probe against the mouse STING mRNA (i.e. *Tmem173*, Cat. No: 413321) was purchased from Advanced Cell Diagnostics. For some experiments, RNAscope signals was combined with immunofluorescence, which was carried out as described below. Images were acquired using the Leica Stellaris 8 confocal microscope or the Keyence BZ-X810 microscope with at least 3 sections from each animal included for data analysis. Cells with more than 5 puncta per cell were classified as positive for STING mRNA expression.

2.6. Immunofluorescence

Mice were deeply anaesthetized with isoflurane and transcardially perfused with PBS followed by 4 % paraformaldehyde (PAF). Lumbar DRG and spinal cord tissues were isolated and post-fixed in PAF for 1–2 h before incubation overnight in a 30 % sucrose solution. Tissues were then embedded in OCT medium (Tissue-Tek) and cryosectioned at a thickness of 14–20 μm. Tissue sections were initially washed with PBS followed by incubation with blocking solution (BSA 1 % and Triton 0.2 % in PBS 1x) for 30 min. After blocking, tissue sections were incubated overnight with the following primary antibodies: anti-IBA-1 (goat, 1:1000, Novus Biologicals, Cat. No: NB1001028), anti-GFAP (mouse, 1:1000, MilliporeSigma, Cat. No: MAB360), anti-NeuN (rabbit, 1:1000, Abcam, Cat. No: Ab177487), and anti-Ki-67 (rabbit, 1:250, Novus Biologicals, Cat. No: NB1001028). The following day, the tissues sections were washed with PBS then incubated for 1 h at room temperature with the following secondary antibodies: anti-goat Alexa Fluor 555 (1:1000, Thermo Fisher Scientific, Cat. No: A21432), anti-mouse Alex Fluor 594 (1:1000, Thermo Fisher Scientific, Cat. No: A11032), and anti-rabbit Alex Fluor 546 (1:1000, Thermo Fisher Scientific, Cat. No: A10040). Images were acquired using the Keyence BZ-X800 microscope.

2.7. Quantitative real-time RT-PCR (qPCR)

DRG and dorsal horn tissues were rapidly removed from terminally anesthetized mice, whereas cells from microglia cultures were harvested with the use of a grinder. Total RNA was extracted from these samples using the Direct-zol RNA MiniPrep kit (Zymo Research, Cat. No: R2053), and its amount and purity were assessed by SimpliNano UV–Vis Spectrophotometer (General Electric). Total RNA was converted into cDNA using a high-capacity cDNA reverse transcription kit (Thermo Fisher Scientific, Cat. No: 4368814). Specific primers used in this study were obtained from PrimerBank (Wang et al., 2012), and their sequences are shown in Suppl. Table 1. qPCR was performed on the QuantStudio 3 Real-Time PCR System (Thermo Fisher Scientific) using PowerUp SYBR Green Master Mix (Thermo Fisher Scientific, Cat. No: A25741). All samples were analyzed at least in duplicate and normalized by glyceraldehyde 3-phosphate dehydrogenase (GAPDH) expression. The relative expression ratio per condition was calculated by the comparative C(T) method (Schmittgen and Livak, 2008).

2.8. RT-PCR

Lumbar dorsal horn tissues were isolated from mice and from a deidentified and non-diseased human donor. Human tissue collection and experiments were approved by the Institutional Review Boards at University of Cincinnati. cDNA was synthesized from these tissues as described above and RT-PCR analysis performed with the following primers: mouse *Tmem173* (forward, 5′-AAATAACTGCCGCCTCATTG-3′; reverse, 5′-ACAGTACGGAGGGAGGAGGT-3′), mouse *Gapdh* (forward, 5′-TGAAGGTCGGTGTGAACGAATT-3′; reverse, 5′-GCTTTCTCCATGGTGG TGAAGA-3′), human TMEM173 (forward, 5′-ACTGTGGGGTGCCTGA-TAAC-3′; reverse, 5′-TGCCCACAGTAACCTCTTCC-3′), and human GAPDH (forward, 5′-ACCCAGAAGACTGTGGATGG-3′; reverse, 5′-TTCTAGACGGCAGGTCAGGT-3′).

2.9. ELISA

An ELISA kit for IFN-β was purchased from R&D systems (Cat# 42410–1, Minneapolis, MN, United States). ELISA was performed using dorsal horn tissues and culture media, and protein concentrations were measured by the Qubit protein assay (Cat# Q33211, Thermo Fisher Scientific). A standard curve was included in each experiment, and IFN-β protein levels measured according to the manufacturer's instruction using a PerkinElmer EnVision plate reader.

2.10. Microglia primary cultures

Microglia cultures were prepared from cerebral cortexes of 2-day-old postnatal mice. Tissues were then minced into approximately 1 mm pieces, triturated, filtered through a 100 μm nylon screen, and collected by centrifugation at approximately 3,000*g* for 5 min. The cell pellets were dissociated with a pipette and resuspended in medium containing 10 % fetal bovine serum in high-glucose DMEM. After trituration, the cells were filtered through a 10 μm screen, plated into T75 flasks, and cultured for 3 weeks. The mixed glia was shaken for 4 h, and the floating cells were collected and subculture at a density of 2.5×10^5 cells/ml. After 1 day of plating, the medium was changed to discharge all non-adherent cells. Some cultures were used for immunofluorescence analysis. Briefly, cultures were incubated with the primary antibody anti-TMEM119 (rabbit, 1:500, Abcam, Cat. No: Ab209064), subsequently with the secondary antibody anti-rabbit Alex Fluor 546 (1:1000, Thermo Fisher Scientific, Cat. No: A10040), and images acquired using the

Keyence BZ-X800 microscope. Immunofluorescence images revealed that only very few plated cells were negative for the microglial marker TMEM119 (Suppl. Fig. 7A). This finding is consistent with qPCR analyses, which showed an enrichment of microglial markers compared to other cell markers in these cultures (Suppl. Fig. 7B). Furthermore, we previously assessed the purity of these cultures to be over 95 % (Berta et al., 2014).

2.11. Statistical analysis

Statistical analysis was performed with Prism 9.0 (GraphPad). All the data are expressed as mean ± standard error (SEM). Biochemical, immunohistochemistry, and behavioral data were analyzed using unpaired Student's *t*-test (two groups) and one-way or two-way ANOVA followed by post-hoc test specified in the figure legends. Statistical details for each experiment are provided in Suppl. Table 4. The criterion for statistical significance was $p < 0.05$. Illustrator 25.0 (Adobe) and BioRender (BioRender.com.) were used for illustrations and figure organization.

3. Results

3.1. Characterization of STING expression in spinal cord of naïve mice

Our current understanding of neuropathic pain is that it arises from plastic changes along the sensory pathway (Fig. 1A). These changes can occur at the level of the primary sensory neurons that transduce the original injury, as well as in the spinal cord, where sensory signaling is often amplified by activated glial cells (Scholz and Woolf, 2007). It was found that STING is expressed in DRG primary sensory neurons and spinal microglia (Donnelly et al., 2021). We confirmed the expression of STING (also known as *Tmem173*) mRNA in mouse and human spinal

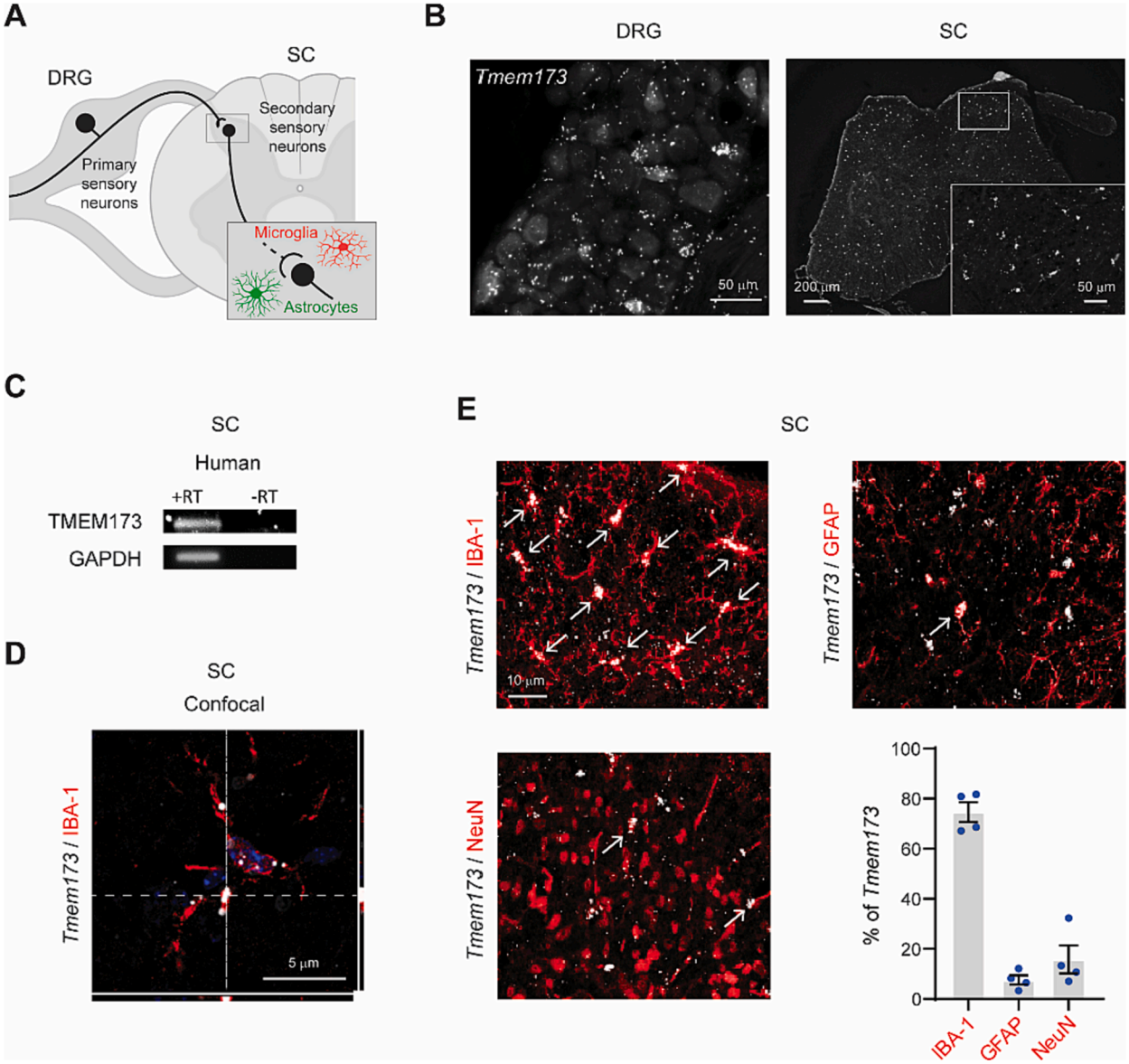

Fig. 1. STING (i.e. TMEM173) expression in spinal microglia. (**A**) Illustration of the sensory pathway involving the transduction of neuropathic pain by DRG primary sensory neurons, its integration by spinal secondary neurons, and its potential amplification by glial cells, such as astrocytes and microglia. (**B**) Representative images of *Tmem173* mRNA expression in DRG and spinal cord tissues from male mice using RNAscope. (**C**) PCR amplification of *Tmem173* mRNA shows expression in spinal cord tissue from a male human donor. RT = reverse transcriptase. (**D**) Confocal orthogonal image of *Tmem173* mRNA expression in IBA-1^{+} microglia. DAPI (blue) is used as nuclei counterstaining. (**E**) Expression and quantification of *Tmem173* mRNA in different cell types labelled by immunohistochemical staining of L4-L5 spinal cord. Arrowheads indicate *Tmem173* mRNA expression in IBA-1 + microglia, GFAP + astrocytes, and NeuN + neurons. n = 4 male mice.

cord tissues (Fig. 1B-C). However, there is conflicting evidence regarding which cell types express STING in the CNS, partly due to nonspecific STING antibodies (Fritsch et al., 2023).

To investigate the cellular locations of STING in the spinal cord, we performed double staining of *Tmem173* mRNA expression by fluorescent RNA *in situ* hybridization (i.e. RNAScope) with immunofluorescence for various cell types (Fig. 1D-E). We found that STING expression is predominantly in microglia cell bodies and processes (Fig. 1D), with *Tmem173* mRNA expressed for 75 % in IBA-1$^+$ microglia, 8 % in GFAP$^+$ astrocytes, and 16 % in NeuN$^+$ neurons (Fig. 1E). This result is consistent with single-cell RNA sequencing analyses, which show that *Tmem173* mRNA expression is prominent in microglia of mouse and human brain (Keren-Shaul et al., 2017; Olah et al., 2020; Olah et al., 2018).

3.2. STING expression is increased in spinal microglia after peripheral nerve injury

To investigate the role of STING in neuropathic pain, we utilized the spared nerve injury (i.e. SNI, Fig. 2A) mouse model (Decosterd and Woolf, 2000). This model is widely used in research because it displays long-lasting mechanical allodynia that is resistant to existing analgesics (Decosterd et al., 2004). We observed an increase in the number of *Tmem173* expressing cells in the ipsilateral dorsal horn of SNI mice compared to naïve male mice (Fig. 2B). Similar increase was observed in female mice, too (data not shown). Expression of *Tmem173* mRNA was predominantly found in IBA-1$^+$ and Ki-67$^+$ proliferating microglia 3 days after SNI (Fig. 2C), and this expression of *Tmem173* persisted in IBA-1$^+$ microglia up to 10 days after SNI (Fig. 2D). We confirmed cell

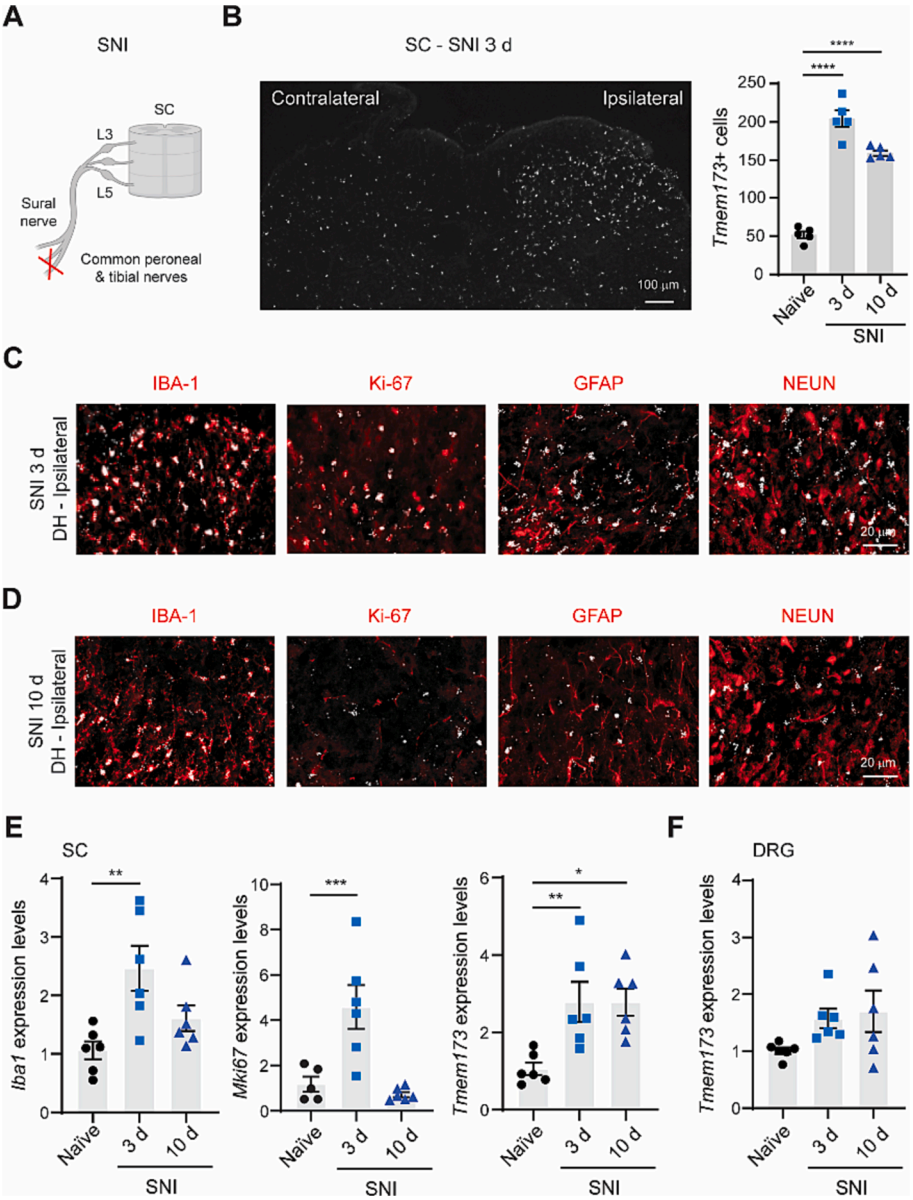

Fig. 2. STING expression in spinal microglia after SNI. (**A**) Illustration of spared nerve injury (SNI), which involves transection and ligation of the common peroneal and tibial nerves, while leaving the sural nerve intact. (**B**) Representative images of Tmem173 mRNA in a lumbar dorsal spinal cord section from a male mouse 3 days after SNI, and quantification of Tmem173 + cells in naïve and SNI mice at 3 and 10 days after surgery. n = 5 male mice, one-way ANOVA, followed by post hoc Dunnett's test, ****p < 0.0001, vs. Naïve. (**C-D**) Expression of *Tmem173* mRNA in different cell types labelled by immunohistochemical staining for IBA-1 + microglia, Ki-67$^+$ proliferative cells, GFAP + astrocytes, and NeuN + neurons at three (C) and ten (D) days after SNI. (**E-F**) qPCR analysis of mRNA expression of Iba1, *Mki67* and *Tmem173* in the ipsilateral lumbar spinal dorsal horn tissues (E), and *Tmem173* in the ipsilateral DRG tissues (F) in naïve and SNI male mice at 3 and 10 after surgery. n = 6 male mice, one-way ANOVA, post hoc Dunnett's test, *p < 0.05, **p < 0.01, ***p < 0.001, vs. Naïve.

proliferation and increased expression of *Tmem173* mRNA in the ipsilateral dorsal horn of SNI mice at three days after SNI using quantitative real-time RT-PCR (qPCR) (Fig. 2E). However, we did not detect any significant change in *Tmem173* mRNA expression in ipsilateral DRG tissue after SNI (Fig. 2D). Our results indicate that SNI induces a significant and sustained increase of STING expression in spinal microglia, which may be linked to the prolonged mechanical allodynia observed in this model.

3.3. STING expression in microglia is not required for mechanical allodynia after peripheral nerve injury

To investigate the potential functional role of STING in microglia after SNI, we used the Tmem119-CreERT2 transgenic mouse line, which allows for specific and inducible genetic manipulations in microglia (Kaiser and Feng, 2019). To validate this mouse line, we crossed the inducible Tmem119-CreERT2 mice with Ai14 reporter mice (Madisen et al., 2010), which progeny express tdTomato after three consecutive days of tamoxifen administration (Suppl. Fig. 1A). Using these mice, we observed tdTomato expression in IBA-1 + microglia in the dorsal horn of the spinal cord, but not in IBA-1 + macrophages in DRG (Suppl. Fig. 1B). Furthermore, we found an ipsilateral increase in *Tmem173* mRNA expression in tdTomato-positive microglia 3 days after SNI (Suppl. Fig. 1C), confirming the specificity and validity of these transgenic mice for our research. To conditionally delete STING from microglia, *Tmem119*-CreERT2 mice were crossed with STING$^{fx/fx}$ mice (Suppl. Fig. 2A). Tamoxifen was administered to these crossed mice to generate microglia-specific conditional knockout mice (STING$^{\Delta MG}$), and to serve as a control, STING$^{fx/fx}$ mice were also treated with tamoxifen (Fig. 3A). Surprisingly, STING$^{\Delta MG}$ mice developed mechanical allodynia similar to the control STING$^{fx/fx}$ mice after SNI, except for a small but significant analgesic effect two days post-surgery (Fig. 3B). We validated the specific decrease in *Tmem173* mRNA expression in spinal dorsal horn, but not DRG tissues, of STING$^{\Delta MG}$ mice compared to STING$^{fx/fx}$ mice (Fig. 3C-E and Suppl. Fig. 2B). We also showed that these mice displayed similar sensorimotor behaviors before and after tamoxifen administration (Suppl. Fig. 2C and Fig. 3F). Previous studies have reported that intrathecal injections of the STING antagonist C-176 significantly reduce mechanical allodynia after SNI (Sun et al., 2022; Wu et al., 2022). We found that intrathecal injections of C-176 significantly but transiently reversed mechanical allodynia ten days after SNI (Suppl. Fig. 2D-E). These data suggest that microglial expression of STING is not required for the development and progression of mechanical allodynia, and intrathecal injections of a STING antagonist appear to have limited therapeutic value.

3.4. STING agonists and IFN-β reduce mechanical allodynia after peripheral nerve injury in male but not female mice

We then asked whether agonists, instead of antagonists, could

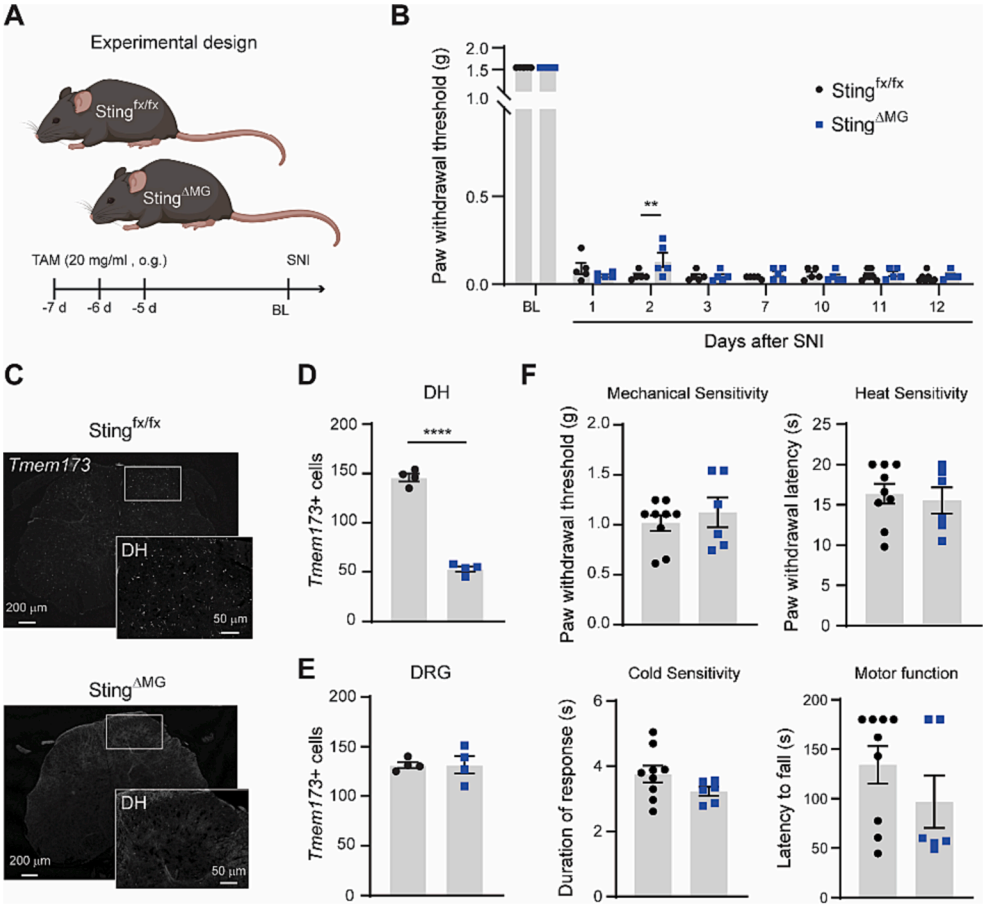

Fig. 3. Microglial STING expression is not required for the development of SNI-induced mechanical allodynia. (**A**) Illustration of the experimental design using the microglia-specific inducible knockout (STING$^{\Delta MG}$) and control (STING$^{fx/fx}$) male mice intraperitoneally injected with tamoxifen. (**B**) Paw withdrawal thresholds were measured in STING$^{\Delta MG}$ and STING$^{fx/fx}$ male mice before (BL = baseline) and after SNI using von Frey filaments to evaluate the development of mechanical allodynia. n = 6 male mice, two-way ANOVA, post hoc Šídák's test, *p < 0.05, vs. STING$^{fx/fx}$. (**C**) Representative *in situ* hybridization image of *Tmem173* mRNA in a lumbar dorsal spinal cord section from STING$^{\Delta MG}$ and STING$^{fx/fx}$ naïve male mice. (**D-E**) Quantification of *Tmem173* positive cells in the spinal dorsal horn (D) and DRG (E) tissues. n = 4 male mice, unpaired *t*-test, ****p < 0.0001, vs. STING$^{fx/fx}$ male mice. (**F**) Assessment of mechanical sensitivity by von Frey filaments, heat sensitivity by Hargreaves test, cold sensitivity by acetone test, and motor function by rotarod in STING$^{\Delta MG}$ (n = 6) and STING$^{fx/fx}$ (n = 9) naïve male mice.

provide a better option for alleviating mechanical allodynia after SNI, as previously reported (Donnelly et al., 2021). ADU-S100 is a specific and potent activator of mouse and human STING and is currently undergoing clinical trials for cancer treatment (Kong et al., 2023). Here, we demonstrate that repeated intrathecal injections of ADU-S100 significantly reversed both early and late mechanical allodynia in male mice after SNI, without apparent tolerance (Fig. 4A-B). However, intrathecal injections of ADU-S100 were ineffective in reversing mechanical allodynia in female mice after SNI (Fig. 4C). Similar results displaying this sex dimorphism were also obtained with systemic injections of ADU-S100 (Suppl. Fig. 3A-B) and intrathecal injections of DMXAA (Suppl. Fig 3C-D), another mouse-specific STING agonist (Conlon et al., 2013). Cold allodynia and pinprick hyperalgesia have also been observed in mice following SNI (Cobos et al., 2018; Li et al., 2023). In our study, we found that repeated intrathecal injections of ADU-S100 (Suppl. Fig 4A) effectively reversed increased withdrawal times in response to dry ice stimulation (Suppl. Fig 4B) and increased frequency of response to pinprick stimulation (Suppl. Fig 4C) in male mice, but not in female mice (Suppl. Fig 4D-E) after SNI. Furthermore, the sex dimorphism by intrathecal injections of ADU-S100 was not specific to the SNI model, as it was also observed for mechanical allodynia in mice with a chronic constriction injury (i.e. CCI, Suppl. Fig. 5A-C), another model of neuropathic pain (Bennett and Xie, 1988). It has been reported that activation of STING in microglia triggers a IFN-I response, which includes the induction of IFN-ß (Mathur et al., 2017). Protein and transcriptional analyses of dorsal horn tissues from the spinal cord of

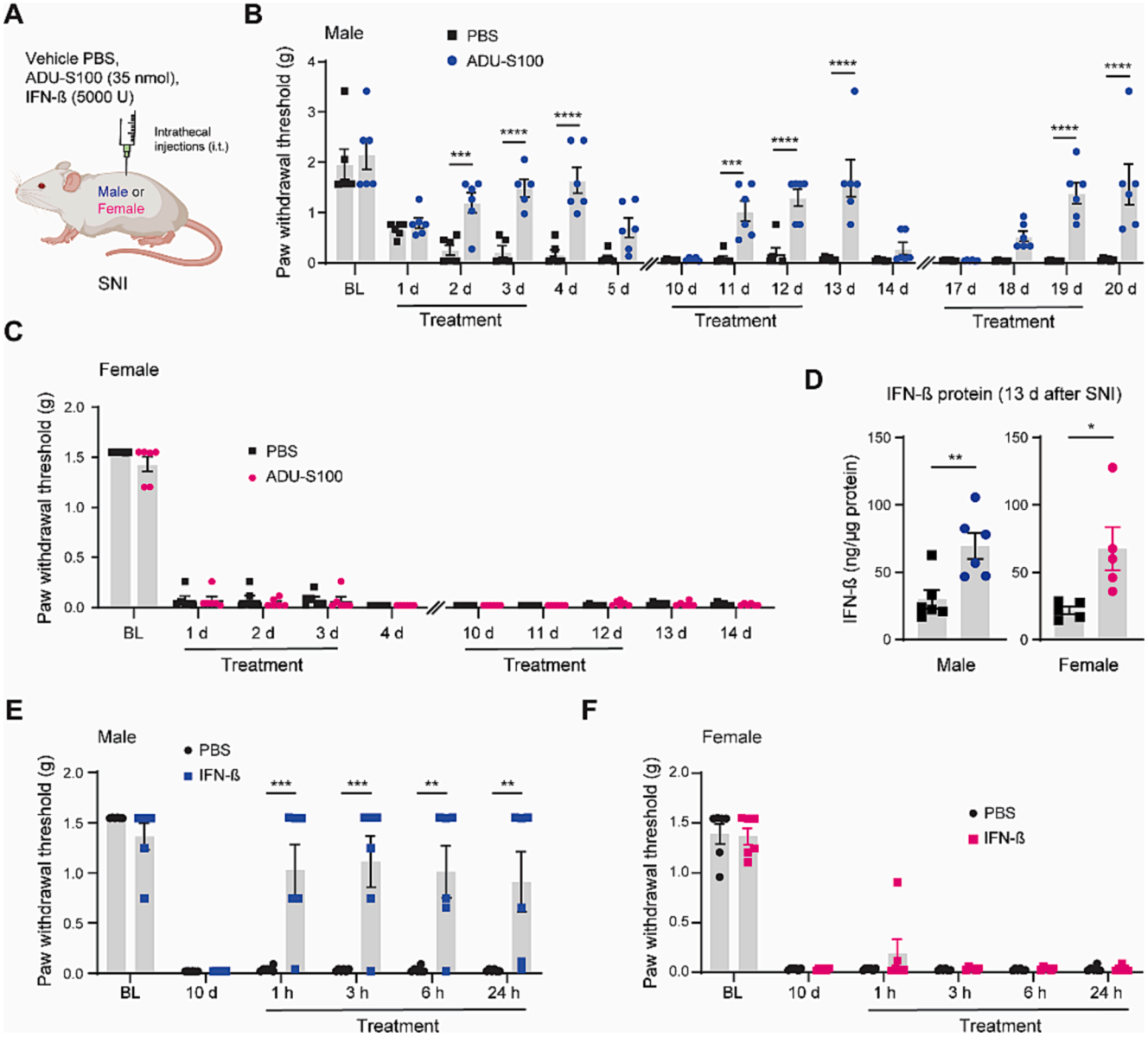

Fig. 4. STING activation and IFN-ß reverse SNI-induced mechanical allodynia in male mice, but not female mice. (**A**) Illustration of the experimental design using intrathecal (i.t.) injections of ADU-S100 and IFN-ß in male and female mice after spared nerve injury (SNI). (**B-C**) Paw withdrawal thresholds were measured before (BL = baseline) and after SNI using von Frey filaments to evaluate the development of mechanical allodynia in male (B) and female (C) mice injected with ADU-S100 or vehicle PBS. n = 6 male mice, two-way ANOVA, post hoc Šídák's test, ***p < 0.001, ****p < 0.0001, vs. PBS; n = 6 female mice, two-way ANOVA, post hoc Šídák's test, vs. PBS. (**D**) Protein levels of IFN-ß in spinal dorsal horn tissues from male and female 13 days after SNI. The mice were injected at day 10, 11 and 12 with ADU-S100 and PBS. n = 6, unpaired *t*-test, *p < 0.05, **p < 0.01, vs. PBS. (**E-F**) Paw withdrawal thresholds were measured before (BL = baseline) and after SNI using von Frey filaments to evaluate the development of mechanical allodynia in male (E) and female (F) mice injected with IFN-ß or control solution. n = 6 male mice, two-way ANOVA, post hoc Šídák's test, **p < 0.01, ***p < 0.001, vs. PBS; n = 6 female mice, two-way ANOVA, post hoc Šídák's test, vs. PBS.

animals treated with ADU-S100 revealed an upregulation of IFN-ß in both male and female mice (Fig. 4D and Suppl. Fig. 6A). Transcriptional analyses also indicated a similar increase of IFN-α and similar expression of IFN receptors in dorsal horn tissues from male and female mice treated with ADU-S100 (Suppl. Fig. 6A-B). This suggests a similar effect of ADU-S100 on the STING-induced IFN-I response in both sexes. However, we observed that intrathecal injection of recombinant IFN-ß significantly reversed mechanical allodynia in male mice after SNI, but not in female mice (Fig. 4E-F), indicating a potential downstream sex-dimorphic effect on IFN-ß.

3.5. *STING activation increases the spinal expression of multiple proinflammatory cytokines after peripheral nerve injury in female mice but not male mice*

STING activation induces not only IFN-I expression but also NF-κB-mediated cytokine production (Balka et al., 2020; Ishikawa and Barber, 2008). To determine if there are any similarities or differences in IFN-I expression and cytokine production between male and female mice, we analyzed the expression of genes associated with these two pathways in the dorsal horn tissues of mice treated with PBS or ADU-S100 after SNI (Fig. 5A). We observed similar regulation of genes associated with IFN-I (e.g., *Irf7* and *Cxcl10*) in both male and female mice, whereas the transcriptional expression of cytokines was predominantly regulated in female mice after ADU-S100 treatment (Fig. 5B and Suppl. Table 2). Specifically, the transcripts of proinflammatory cytokines IL-1β, TNFα, and CCL2 (chemokine ligand 2) showed significant increases only in female mice treated with ADU-S100, compared to those treated with PBS (Fig. 5C). These effects may be due to different activation of spinal glial cells (Ji et al., 2013). However, the transcripts associated with activation of astrocytes (i.e. *Gfap*) and microglial activation (i.e. *Cd11b*) were not altered by ADU-S00 treatment in both male and female mice (Fig. 5D). CD11c-expressing spinal microglia may contribute to pain recovery mechanism after peripheral nerve injury (Kohno et al., 2022). ADU-S100 may alleviate pain in male mice by increasing CD11c-expressing microglia. Surprisingly, *Cd11c* transcripts were significantly increased only in female mice after ADU-S100 administration (Fig. 5D). This suggests a more complex underlying mechanism for the analgesic effect of ADU-S100, warranting further studies. Overall, these data indicate that activation of STING by ADU-S100 leads to similar expression of IFN-I but differing production of proinflammatory cytokines between male and female mice.

3.6. *Microglial activation of STING is required to reduce mechanical allodynia after peripheral nerve injury*

Next, we investigated whether the analgesic effect of ADU-S100 depends on the presence of STING expression in microglia, using $STING^{\Delta MG}$ and $STING^{fx/fx}$ mice. Although the expression of STING appears to have little impact on the development of mechanical allodynia (Fig. 3B), we used two strategies involving tamoxifen-induced Cre recombination, before and after SNI, respectively, to allow for the development of mechanical allodynia in the presence of STING or in its absence (Fig. 6A). With both strategies, intrathecal injections of ADU-S100 were ineffective in reversing established mechanical allodynia in $STING^{\Delta MG}$ mice, compared to $STING^{fx/fx}$ mice after SNI (Fig. 6B). This suggests a requirement of microglial STING expression for the analgesic effect of ADU-S100. To further investigate the analgesic role of

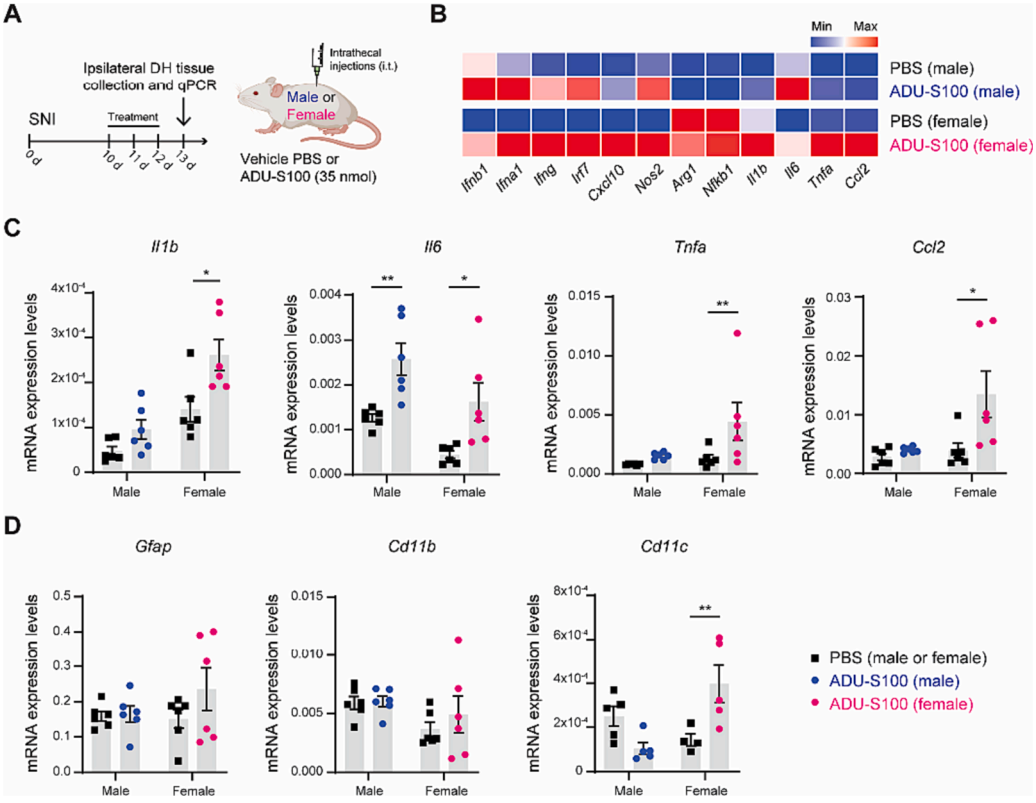

Fig. 5. STING activation leads to increased levels of multiple proinflammatory cytokines after SNI in spinal dorsal horn tissue from female mice, but not from male mice. (**A**) Illustration of the experimental design using intrathecal (i.t.) injections of vehicle PBS or ADU-S100 (35 nmol) 10 d after SNI in male and female mice. (**B**) Heatmap summarizing the expression of genes associated with IFN-I signaling and NF-κB-induced cytokine production (to note, values used to generate this heatmap are included in Supplementary Table 2). (**C**) Histograms of qPCR analyses of proinflammatory cytokines *Il1b*, *Il6*, *Tnfa*, and *Ccl2*. n = 6 per group, uncorrected Fisher's LSD, *p < 0.05, **p < 0.01, vs. PBS. (**D**) Histograms of qPCR analyses of genes associated with the activation of astrocytes (i.e. *Gfap*) and microglia (i.e. *Cd11b*), as well as microglial pain recovery (i.e. *Cd11c*). n = 4–6 per group, uncorrected Fisher's LSD, **p < 0.01, vs. PBS.

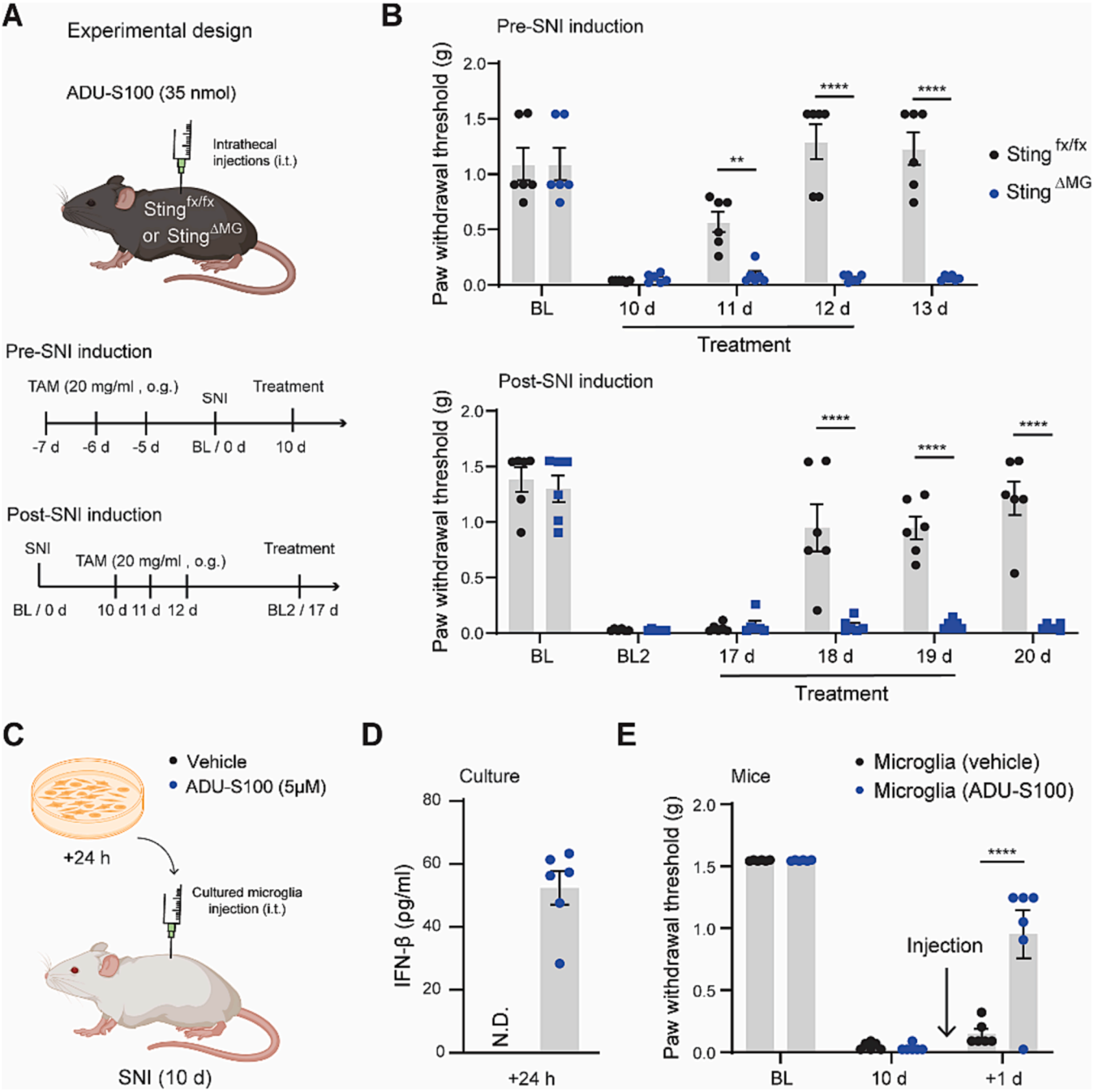

Fig. 6. Microglial STING activation is required to reverse SNI-induced mechanical allodynia. (**A**) Illustration of the experimental design using intrathecal (i.t.) injections of ADU-S100 in STING$^{\Delta MG}$ and STING$^{fx/fx}$ male mice. (**B**) Paw withdrawal thresholds were measured before (BL = baseline) and after SNI using von Frey filaments to evaluate the development of mechanical allodynia in mice injected with tamoxifen pre- (upper panel) and post-SNI (lower panel), and treated with ADU-S100 for three consecutive days. n = 6 male mice, two-way ANOVA, post hoc Šídák's test, ****$p < 0.0001$, vs. STING$^{fx/fx}$. (**C**) Illustration of the experimental design using cell cultures and intrathecal injections of these cells in male mice 10 days after SNI. (**D**) Protein analysis of IFN-ß in culture media from microglia treated with control vehicle and ADU-S100. To note, IFN-ß was not detected (N.D.) in media from microglia treated with a vehicle. (**E**) Paw withdrawal thresholds were measured before (BL = baseline) and 10 days after SNI using von Frey filaments to evaluate the development of mechanical allodynia in male mice injected with microglial cells treated with control vehicle and ADU-S100. n = 6 male mice, two-way ANOVA, post hoc Šídák's test, ****$p < 0.0001$, vs. vehicle.

microglial STING activation and release of IFN-ß, we incubated microglial cell cultures with ADU-S100 or a control vehicle, and then intrathecally injected these cells in male mice to assess their effect on SNI-induced mechanical allodynia (Fig. 6C). Although microglia cell cultures display different molecular signatures and morphology when compared with in vivo microglia (Dubbelaar et al., 2018), these cultures treated with ADU-S100 for 24 h (Suppl. Fig. 7C) showed a clear IFN-I response (Suppl. Fig. 7E-G and Suppl. Table 3), similar to that observed in male mice after SNI and ADU-S100 treatment (Fig. 5). Furthermore, they exhibited production and release of IFN-ß (Fig. 6D). More importantly, we found that mechanical allodynia was significantly reversed in mice that received ADU-S100 treated microglial cells, but not in mice with vehicle-treated cells (Fig. 6E). Our previous studies have suggested that STING expression in Nav1.8-expressing nociceptive peripheral sensory neurons plays an important role in driving both acute and chronic pain (Donnelly et al., 2021; Wang et al., 2021). To

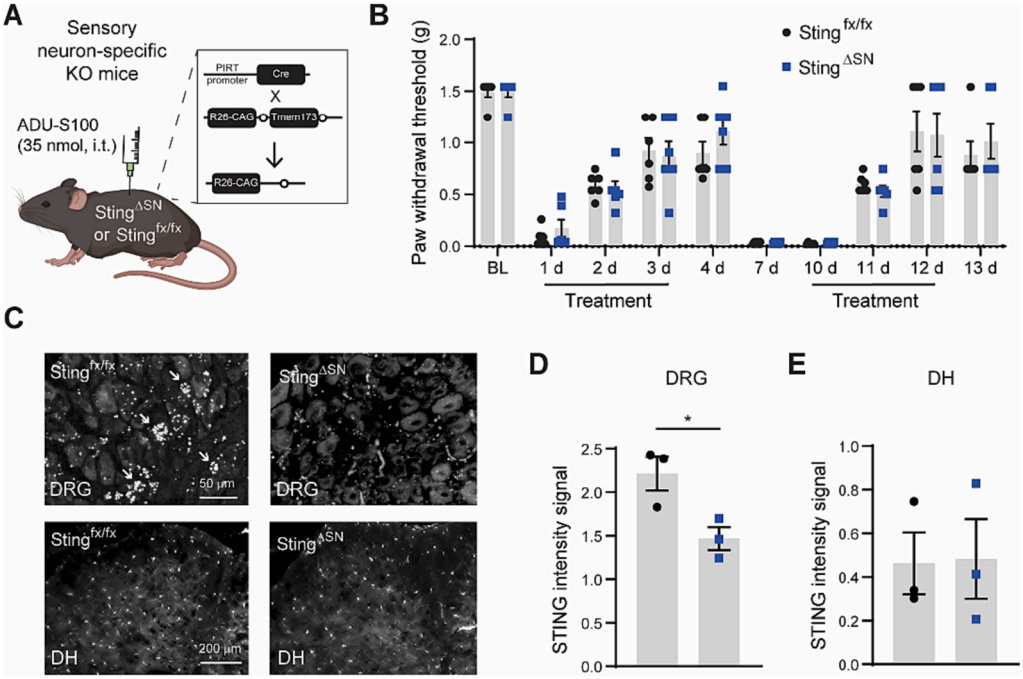

Fig. 7. STING activation in sensory neurons is not required to reverse SNI-induced mechanical allodynia. (**A**) Illustration of the experimental design using intrathecal (i.t.) injections of ADU-S100 and mating strategy for inducing sensory neuron-specific inducible knockout (STING$^{\Delta SN}$) mice. Pirt-Cre; STING$^{fx/fx}$ male mice were used. (**B**) Paw withdrawal thresholds were measured before (BL = baseline) and after SNI using von Frey filaments to evaluate the development of mechanical allodynia in STING$^{\Delta SN}$ and STING$^{fx/fx}$ male mice treated with ADU-S100. n = 6 male mice. (**C**) Representative *in situ* hybridization image of *Tmem173* mRNA in a lumbar DRG and dorsal horn (DH) sections from STING$^{\Delta SN}$ and STING$^{fx/fx}$ naïve male mice. (**D-E**) Quantification of *Tmem173* mRNA positive cells in DRG (D) and DH (E) tissues from male mice. n = 3, unpaired *t*-test, *p < 0.05, vs. STING$^{fx/fx}$.

investigate the potential role in the analgesic effect of ADU-S100 of STING expression in sensory neurons, we generated sensory neuron-specific conditional knockout mice (STING$^{\Delta SN}$) by crossing STING$^{fx/fx}$ mice with Pirt-Cre mice (Fig. 7A). Pirt-Cre mice are used for genetic manipulation of most peripheral sensory neurons, including nociceptors and mechanoreceptors (Kim et al., 2016; Zheng et al., 2022).

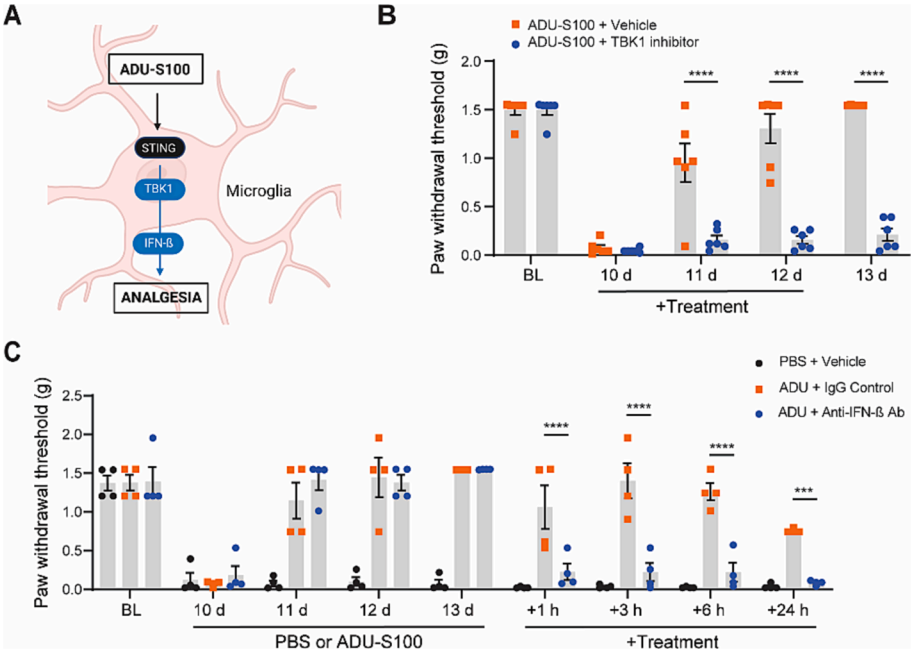

Fig. 8. STING activation reduces mechanical allodynia via TBK1 and IFN-ß signaling. (**A**) Schematic showing that STING downstream signaling (i.e. TBK1 and IFN-ß) (**B**) Paw withdrawal thresholds were measured before (BL = baseline) and after SNI using von Frey filaments to evaluate the development of mechanical allodynia in male mice injected with ADU-S100 with a control vehicle or TBK1 inhibitor GSK8612 (20 mg/kg). n = 6 male mice, two-way ANOVA, post hoc Šídák's test, ****p < 0.0001, vs. vehicle. (**C**) Paw withdrawal thresholds were measured before (BL = baseline) and after SNI using von Frey filaments to evaluate the development of mechanical allodynia in male mice injected with ADU-S100 or PBS for three consecutive days and then intrathecally treated with 10 μg of IgG controls or anti-IFN-ß antibody (Ab). n = 6 male mice, two-way ANOVA, post hoc Šídák's test, ***p < 0.001, ****p < 0.0001, vs. IgG control.

Interestingly, we observed that STING$^{\Delta SN}$ mice developed mechanical allodynia similar to control STING$^{fx/fx}$ mice after SNI. Moreover, the analgesic effect of ADU-S100 was maintained in these mice (Fig. 7B). We also confirmed the specific decrease in Tmem173 mRNA expression in DRG sensory neurons of STING$^{\Delta SN}$ mice compared to STING$^{fx/fx}$ mice, but not in SC tissues (Fig. 7C-E). These findings suggest that the analgesic effect of ADU-S100 after SNI requires activation of STING in microglia, but not in sensory neurons.

3.7. STING activation reduces mechanical allodynia via TBK1 and IFN-β signaling

It is well known that activation of STING is often followed by the engagement of TBK1 and IRF3 (Barber, 2014; Ishikawa et al., 2009), resulting in an IFN-I response including the production of IFN-ß (Fig. 8A). Since this response is highly dependent on TBK1 activity (Balka et al., 2020), we tested whether TBK1 had an impact on the analgesic effect of ADU-S100 after SNI. Our results showed that daily intraperitoneal injections of GSK8612, a selective and potent TBK1 inhibitor (Thomson et al., 2019), abolished the analgesic effect of ADU-S100 on days 11, 12, and 13 after SNI (Fig. 8B). Furthermore, we have shown that this effect depends on the release of IFN-ß. The analgesic effect of ADU-S100 at day 13 after SNI was also abolished by intrathecal injection of a neutralizing IFN-ß antibody (Fig. 8C). Together these findings indicate that STING activation has analgesic effect that relies on downstream signaling including the activation of TBK1 and the production of IFN-ß.

4. Discussion

Neuropathic pain is a debilitating condition that is difficult to treat with current analgesics (Grosser et al., 2017). Following peripheral nerve injury, spinal microglia proliferate and play a crucial role in the development and maintenance of neuropathic pain through PRR signaling and release of proinflammatory cytokines (Ji et al., 2013). For instance, toll-like receptors (TLRs) are well-known PRRs expressed in microglia, and their inhibition can effectively reduce neuropathic pain (Lacagnina et al., 2018). However, recent studies have uncovered a more nuanced understanding of the role of microglia in neuropathic pain (Chen et al., 2018). These studies suggest that microglia can have sexually dimorphic effects (Sorge et al., 2015; Tansley et al., 2022; Taves et al., 2016) and can also play a beneficial role in the prevention and resolution of neuropathic pain (Kohno et al., 2022; McKelvey et al., 2015). In this study, we show that STING, another PRR (Ishikawa and Barber, 2008), is abundantly expressed in spinal microglia and is increased ipsilaterally after peripheral nerve injury. However, microglial expression of STING is not necessary for the development of nerve injury-induced mechanical allodynia, a common symptom of neuropathic pain. Consistent with this finding, inhibiting STING using the specific STING agonist C-176 has little to no effect on reducing mechanical allodynia. Conversely, activating STING in microglia through intrathecal injections of ADU-S100 and DMXAA, two STING agonists currently being tested in clinical trials, significantly alleviated both allodynia and hyperalgesia in male mice, but not female mice. This effect likely involves TBK1 activation and IFN-ß production, although additional work will be necessary to better understand these downstream signaling pathways.

Using RNAScope, we have demonstrated that STING transcripts are predominantly expressed in spinal microglial cells, although they are present in a few spinal astrocytes and neurons as well. This distribution is consistent with RNA-seq data of various cells in the brain (Zhang et al., 2014). Additionally, we have previously shown STING expression in mouse peripheral sensory neurons and spinal microglia (Donnelly et al., 2021). Other studies have observed high expression of STING in rat spinal neurons by immunofluorescence (Sun et al., 2022; Wu et al., 2022). Recent studies have also shown an increase in STING expression in microglia after peripheral nerve injury, consistent with our findings. Nonetheless, the functional role of microglial increased expression of STING in neuropathic pain is still under debate. This is partly due to its widespread expression in multiple cells of both the peripheral and central nervous system (Hu et al., 2023; Yang et al., 2022).

To investigate the functional role of STING specifically in microglia, we used Cre/LoxP technology, which allows for the silencing of gene expression in specific cell types (McLellan et al., 2017). The fractalkine receptor CX3CR1 promoter is commonly used for this purpose in microglia-specific Cre lines (Goldmann et al., 2013). However, its use may lead to confounding results since CX3CR1 is also expressed in peripheral tissue macrophages that contribute to neuropathic pain (Chen et al., 2020; Yu et al., 2020). Therefore, we opted to use the recently developed microglia-specific *Tmem119*-CreERT2 transgenic mouse line (Kaiser and Feng, 2019), which we confirm does not drive recombination in peripheral DRG tissue and macrophages. We thus generated mice with an inducible microglia-targeting *Tmem173* conditional knockout (STING$^{\Delta MG}$) by crossing STING$^{fx/fx}$ mice with the *Tmem119*-CreERT2 mouse line. We found that microglial expression of STING does not modulate nociception and motor function in naïve mice and, surprisingly, is not required for the development and maintenance of mechanical allodynia in male mice after SNI. Despite its increase in microglia after SNI, STING may remain latent as its activation depends on the regulation of several signaling pathways (Decout et al., 2021). A study has reported the potential involvement of STING expression in microglia reactivity and neuroinflammation (Mathur et al., 2017). However, we found that STING activation in male mice after SNI does not changes most proinflammatory cytokines or marker of glial cell activation associated with neuroinflammation. Other studies have suggested that the cGAS-STING pathway is activated after SNI, and reported that repeated intrathecal administrations of inhibitors for cGAS (i.e. RU.521) and STING (i.e. C-176) reversed mechanical allodynia in rats after SNI. Notably, these inhibitors may engage different signaling pathway involving the blockade of NF-kB and proinflammatory cytokines (Sun et al., 2022; Wu et al., 2022). In our study, we found that a similar dose of C-176 used in these studies partially and temporarily attenuated SNI-induced mechanical allodynia. However, we were unable to demonstrate the reversal of this allodynia by repeated intrathecal administrations. When we used a 100X higher dose of the inhibitor, we observed the reversal of mechanical allodynia, but mice displayed clear discomfort and unhealthy behaviors (data not shown). We conclude that microglial expression of STING is not necessary for the development and maintenance of mechanical allodynia after nerve injury and that STING inhibition seems to have limited therapeutic value. However, it's worth noting that our and other's studies included different species and time courses of drug administration, which require further investigation.

Previously, we reported that the intrathecal administration of STING agonists (i.e. ADU-S100 or DMXAA) relieved mechanical allodynia in mice after SNI through IFN-I signaling (Donnelly et al., 2021). Here, we confirmed this report and demonstrated that repeated intrathecal administrations of ADU-S100 significantly reversed mechanical allodynia in male mice after SNI, without showing sign of tolerance. ADU-S100 also reversed cold allodynia and pinprick hyperalgesia in male mice after SNI. However, we found that the same intrathecal administrations were ineffective in reversing these behaviors in female mice after SNI. Notably, this difference in STING activation between sexes was also observed when using another STING agonist (DMXAA), as well as in another mouse model of neuropathic pain (CCI). Sexual dimorphism may arise from varying levels of activation of STING and its downstream signaling, such as IFN-I signaling (Tan et al., 2021), between male and female mice. A recent single-cell RNA sequencing of mouse spinal cord microglia after nerve injury revealed a transitory, but significant increase in interferon and cytokine-mediated signaling in male mice, but not in female mice (Tansley et al., 2022). We found that repeated administration of the STING agonist ADU-S100 equally increased transcriptional expression and protein levels of IFN-ß in both sexes.

However, when recombinant IFN-ß protein was administered intrathecally, it only reversed SNI-induced mechanical allodynia in male mice. This suggests a sexual dimorphism in the spinal STING downstream signaling, specifically related to IFN-ß, following nerve injury. One possible explanation for this difference could be a different expression and regulation of spinal IFN-I receptors. However, both *Ifnar1* and *Ifnar2* mRNAs showed similar expression in the dorsal horn tissue of male and female mice and were not affected by ADU-S100.

Type I interferons, such as IFN-ß, have contradictory effects on pain. While some studies suggest they act as pain inducers (Barragán-Iglesias et al., 2020; Lin et al., 2020), we and others suggest they have pain-relieving effects (Donnelly et al., 2021; Liu et al., 2016; Liu et al., 2020; Stokes et al., 2013; Tan et al., 2012; Woller et al., 2019). This contradiction may stem from the different actions of interferons in the peripheral and central nervous systems (Tan et al., 2021). Consistent with our findings, multiple studies have reported that spinal administration of IFN-α/ß generally has analgesic effects in animal models of both inflammatory and neuropathic pain (Donnelly et al., 2021; Liu et al., 2016; Liu et al., 2020; Stokes et al., 2013; Tan et al., 2012; Wang et al., 2021; Woller et al., 2019). However, most of the studies only included male animals. None of them reported or focused on sex differences in the analgesic actions of IFN-α/ß, despite the fact that IFN-Is are known to modulate antiviral immunity in a sex-specific manner (Pujantell and Altfeld, 2022). It has also been reported that type I IFN may play a role in mediating sex differences in cytokine production after viral signaling activation in the central nervous system (Posillico et al., 2021). Consistent with this report, our findings indicate that activation of STING by ADU-S100 leads to similar expression of IFN-I but different production of proinflammatory cytokines in male and female mice. In male mice, no significant changes were observed in the expression of proinflammatory cytokines, except for IL-6 mRNA. This suggests that the analgesic effect of ADU-S100 may be due to the induction of IFN-I rather than the suppression of neuroinflammation. In contrast, female mice treated with ADU-S100 show significant increases in proinflammatory cytokines IL-1ß, TNFα, and CCL2 mRNAs compared to male mice. It is tempting to suggest that proinflammatory and algesic cytokines, such as IL-1ß, may counteract the analgesic effects of ADU-S100 (Berta et al., 2012). Overall, these data highlight the complex underlying mechanisms of ADU-S100′s analgesic effects, which certainly warrant further studies.

Microglia are well-known to produce IFN-Is upon cGAS/STING activation (Gulen et al., 2023; Mathur et al., 2017; Udeochu et al., 2023). Therefore, it is worth investigating whether the analgesic effect of ADU-S100 is dependent on microglial expression of STING. Our study using the $STING^{\Delta MG}$ mice shows that the analgesic effect of ADU-S100 requires the expression of STING in microglia. To further confirm the analgesic effect of ADU-S100 after nerve injury via microglia, we showed that intrathecal injection of microglial culture stimulated with ADU-S100 was enough to reverse mechanical allodynia caused by SNI. Although these microglia do not integrate into the spinal cord, they release IFNß, which can penetrate the spinal tissue. Validating this approach and results, we demonstrated that stimulating microglial culture with ADU-S100 induced significant transcriptional responses in IFN-I signaling, similar to what was observed in male mice after SNI and treatment with ADU-S100. Previous studies have also demonstrated similar microglial IFN signaling responses upon cGAS/STING activation by the antiviral drug ganciclovir (Mathur et al., 2017). Our previous data indicated that STING-mediated IFN signaling may act through an autocrine and/or paracrine mechanism in peripheral sensory neurons (Donnelly et al., 2021), suggesting a potential role of these neurons in the development of neuropathic pain and the analgesic effect of ADU-S100. However, we observed that $STING^{\Delta SN}$ (i.e. peripheral sensory neuron-specific conditional knockout) mice developed mechanical allodynia similar to control $STING^{fx/fx}$ mice after SNI. Moreover, the analgesic effect of ADU-S100 was maintained in these mice. These findings suggest that the development of neuropathic pain after nerve injury may not require the expression of STING in peripheral sensory neurons or microglia. However, the analgesic effect of ADU-S100 after SNI requires activation of STING in microglia, but not in peripheral sensory neurons.

Mechanistically, the engagement of the cGAS/STING pathway activates the kinase TBK1, which is critical for transcribing downstream effector genes, including IFN-ß (Balka et al., 2020). Our study found that spinal inhibition of TBK1 or IFN-ß largely abolished the analgesic effect of ADU-S100 after SNI. Although our work contributes to the growing understanding of the potential mechanisms by which spinal IFN-ß may attenuate pain, such as through the suppression of sodium and calcium channel function in primary sensory neurons (Donnelly et al., 2021) and the inhibition of spinal mitogen-activated protein kinases (Liu et al., 2020), the underlying mechanisms are complex and require further investigation. Additionally, there are important limitations in our study that must be considered. First, we have focused on IFN-ß, but ADU-S100′s STING activation also induces IFN-α (Donnelly et al., 2021). We have previously reported that both IFN-α and IFN-ß have analgesic effects in animal models of inflammatory and neuropathic pain (Donnelly et al., 2021; Tan et al., 2012). Consistently, spinal IFN-α has an anti-nociceptive effect through the mu opioid receptors (Jiang et al., 2000). However, others have suggested that IFN-α may have a pro-nociceptive role by enhancing spinal excitatory transmission (Qin et al., 2012). Further studies are needed to understand the spinal actions of IFN-α and IFN-ß, as their analgesic effects may depend on the regulation of other cytokines (Woller et al., 2019). Second, we evaluated the anti-nociceptive effects of STING activation on nerve-injury-induced mechanical allodynia, cold allodynia, and pinprick hyperalgesia. However, neuropathic pain is a complex condition that involves both sensory and emotional components (Talbot et al., 2019). Therefore, future studies should investigate how ADU-S100 affects different components of neuropathic pain, particularly since our intrathecal administration and genetic approach can target brain regions where microglial STING activation may contribute to both sensory and emotional pain (Hu et al., 2023; Zhang et al., 2022). Third, it is important to note that STING agonists present new therapeutic opportunities, but also pose challenges (Motedayen Aval et al., 2020). Differences in species and single nucleotide polymorphisms in STING can affect the choice of appropriate STING agonists. For example, DMXAA is specific to mouse STING, despite sharing 68 % amino acid identity with human STING (Shih et al., 2018). On the other hand, ADU-S100 and its derivatives can activate both mouse and human STING, and advanced to clinical trials for cancer treatment (Kim et al., 2021; Meric-Bernstam et al., 2022; Meric-Bernstam et al., 2023). However, it is essential to define the safe dosing of STING agonists and use local administrations to minimize the risks of immunotoxicity and tolerogenic responses (Ahn et al., 2014; Huang et al., 2013). In our study, we administered STING agonists through intrathecal injections, which limits their spread into the CNS but can present practical challenges in a clinical setting (Berta et al., 2023). Nevertheless, this route has been approved and used in clinic for delivering morphine and ziconotide to treat severe chronic pain (Chalil et al., 2021).

Overall, our study highlights the potential therapeutic value of activating STING in microglia for the treatment of neuropathic pain. While microglial expression of STING is not necessary for the development and maintenance of mechanical allodynia after nerve injury, activating STING in microglia via intrathecal injections of ADU-S100 significantly alleviated mechanical allodynia in male mice through IFN-ß signaling. ADU-S100 also reduced cold allodynia and pinprick hyperalgesia in male mice after SNI. However, the pain-relieving effects of ADU-S100 and IFN-ß were not observed in female mice. This could be attributed to a potential sexual dimorphism in STING activation following nerve injury, leading to a higher production of proinflammatory cytokines in female mice that may counteract the analgesic effect of ADU-S100 and IFN-ß. Further investigations are required to better understand the mechanisms, safety, and effectiveness of STING

agonists. Nevertheless, these findings offer a promising avenue for potential clinical treatment of neuropathic pain.

CRediT authorship contribution statement

Arthur Silveira Prudente: . **Sang Hoon Lee:** . **Jueun Roh:** Investigation, Methodology, Validation, Visualization. **Debora D. Luckemeyer:** Investigation, Methodology, Validation. **Cinder Faith Cohen:** . **Marie Pertin:** Investigation, Validation. **Chul-Kyu Park:** Supervision, Writing – review & editing. **Marc R. Suter:** Supervision, Writing – review & editing. **Isabelle Decosterd:** Supervision, Writing – review & editing. **Jun-Ming Zhang:** Supervision, Writing – review & editing. **Ru-Rong Ji:** Conceptualization, Supervision, Writing – review & editing. **Temugin Berta:** Conceptualization, Data curation, Formal analysis, Funding acquisition, Supervision, Writing – original draft.

Declaration of competing interest

The authors declare that they have no known competing financial interests or personal relationships that could have appeared to influence the work reported in this paper.

Data availability

Data will be made available on request.

Acknowledgements

This study is supported by the US National Institutes of Health (NIH) R01 grants NS113243 (T.B.), DE17794 (R.-R.J.) and NS045594 (J.-M. Z.), and NIH R21 grant NS121946 (T.B.). This study was also partially supported by the National Research Foundation (NRF) of Korea grant NRF-2022M3E5E8081191 (C.-K.P.).

Author contributions

A.S.P. and T.B. developed the project. A.S.P and S.H.L. conducted most of the experiments and/or data analyses with J.R., D.D.L., C.F.C., M.P., C.K.P., M.R.S., I.D., J.-M.Z., R.-R.J., and T.B. providing assistance. A.S.P. and T.B. wrote the manuscript. R.-R.J. and M.R.S. and other co-authors edited the manuscript. All authors approved the final manuscript submission.

Data sharing

Data will be made available on request to the lead contact T.B. (temugin.berta@uc.edu).

Appendix A. Supplementary data

Supplementary data to this article can be found online at https://doi.org/10.1016/j.bbi.2024.01.003.

References

Ahn, J., Xia, T., Konno, H., Konno, K., Ruiz, P., Barber, G.N., 2014. Inflammation-driven carcinogenesis is mediated through STING. Nat. Commun. 5, 5166.
Balka, K.R., Louis, C., Saunders, T.L., Smith, A.M., Calleja, D.J., D'Silva, D.B., Moghaddas, F., Tailler, M., Lawlor, K.E., Zhan, Y., Burns, C.J., Wicks, I.P., Miner, J. J., Kile, B.T., Masters, S.L., De Nardo, D., 2020. TBK1 and IKKε act redundantly to mediate STING-induced NF-κB responses in myeloid cells. Cell Rep. 31, 107492.
Barber, G.N., 2014. STING-dependent cytosolic DNA sensing pathways. Trends Immunol. 35, 88–93.
Barragán-Iglesias, P., Franco-Enzástiga, Ú., Jeevakumar, V., Shiers, S., Wangzhou, A., Granados-Soto, V., Campbell, Z.T., Dussor, G., Price, T.J., 2020. Type I interferons act directly on nociceptors to produce pain sensitization: implications for viral infection-induced pain. J. Neurosci. 40, 3517–3532.
Bennett, G.J., Xie, Y.K., 1988. A peripheral mononeuropathy in rat that produces disorders of pain sensation like those seen in man. Pain 33, 87–107.
Berta, T., Liu, T., Liu, Y.C., Xu, Z.Z., Ji, R.R., 2012. Acute morphine activates satellite glial cells and up-regulates IL-1β in dorsal root ganglia in mice via matrix metalloprotease-9. Mol. Pain 8, 18.
Berta, T., Park, C.K., Xu, Z.Z., Xie, R.G., Liu, T., Lü, N., Liu, Y.C., Ji, R.R., 2014. Extracellular caspase-6 drives murine inflammatory pain via microglial TNF-α secretion. J. Clin. Invest. 124, 1173–1186.
Berta, T., Perrin, F.E., Pertin, M., Tonello, R., Liu, Y.C., Chamessian, A., Kato, A.C., Ji, R. R., Decosterd, I., 2017. Gene expression profiling of cutaneous injured and non-injured nociceptors in SNI animal model of neuropathic pain. Sci. Rep. 7, 9367.
Berta, T., Strong, J.A., Zhang, J.M., Ji, R.R., 2023. Targeting dorsal root ganglia and primary sensory neurons for the treatment of chronic pain: an update. Expert Opin. Ther. Targets 1–14.
Brenner, D.S., Golden, J.P., Gereau, R.W.T., 2012. A novel behavioral assay for measuring cold sensation in mice. PLoS One 7, e39765.
Burdette, D.L., Vance, R.E., 2013. STING and the innate immune response to nucleic acids in the cytosol. Nat. Immunol. 14, 19–26.
Chalil, A., Staudt, M.D., Harland, T.A., Leimer, E.M., Bhullar, R., Argoff, C.E., 2021. A safety review of approved intrathecal analgesics for chronic pain management. Expert Opin. Drug Saf. 20, 439–451.
Chaplan, S.R., Bach, F.W., Pogrel, J.W., Chung, J.M., Yaksh, T.L., 1994. Quantitative assessment of tactile allodynia in the rat paw. J. Neurosci. Methods 53, 55–63.
Chen, O., Donnelly, C.R., Ji, R.R., 2020. Regulation of pain by neuro-immune interactions between macrophages and nociceptor sensory neurons. Curr. Opin. Neurobiol. 62, 17–25.
Chen, G., Zhang, Y.Q., Qadri, Y.J., Serhan, C.N., Ji, R.R., 2018. Microglia in Pain: Detrimental and Protective Roles in Pathogenesis and Resolution of Pain. Neuron 100, 1292–1311.
Chin, A.C., 2019. Neuroinflammation and the cGAS-STING pathway. J. Neurophysiol. 121, 1087–1091.
Cobos, E.J., Nickerson, C.A., Gao, F., Chandran, V., Bravo-Caparrós, I., González-Cano, R., Riva, P., Andrews, N.A., Latremoliere, A., Seehus, C.R., Perazzoli, G., Nieto, F.R., Joller, N., Painter, M.W., Ma, C.H.E., Omura, T., Chesler, E.J., Geschwind, D.H., Coppola, G., Rangachari, M., Woolf, C.J., Costigan, M., 2018. Mechanistic differences in neuropathic pain modalities revealed by correlating behavior with global expression profiling. Cell Rep. 22, 1301–1312.
Conlon, J., Burdette, D.L., Sharma, S., Bhat, N., Thompson, M., Jiang, Z., Rathinam, V.A. K., Monks, B., Jin, T., Xiao, T.S., Vogel, S.N., Vance, R.E., Fitzgerald, K.A., 2013. Mouse, but not human STING, binds and signals in response to the vascular disrupting agent 5,6-dimethylxanthenone-4-acetic acid. J. Immunol. 190, 5216–5225.
Decosterd, I., Woolf, C.J., 2000. Spared nerve injury: an animal model of persistent peripheral neuropathic pain. Pain 87, 149–158.
Decosterd, I., Allchorne, A., Woolf, C.J., 2004. Differential analgesic sensitivity of two distinct neuropathic pain models. Anesth. Analg. 99, 457–463 table of contents.
Decout, A., Katz, J.D., Venkatraman, S., Ablasser, A., 2021. The cGAS-STING pathway as a therapeutic target in inflammatory diseases. Nat. Rev. Immunol. 21, 548–569.
Dixon, W.J., 1980. Efficient analysis of experimental observations. Annu. Rev. Pharmacol. Toxicol. 20, 441–462.
Donnelly, C.R., Jiang, C., Andriessen, A.S., Wang, K., Wang, Z., Ding, H., Zhao, J., Luo, X., Lee, M.S., Lei, Y.L., Maixner, W., Ko, M.C., Ji, R.R., 2021. STING controls nociception via type I interferon signalling in sensory neurons. Nature 591, 275–280.
Dubbelaar, M.L., Kracht, L., Eggen, B.J.L., Boddeke, E.W.G.M., 2018. The kaleidoscope of microglial phenotypes. Front. Immunol. 9.
Eisenach, J.C., Curry, R., Tong, C., Houle, T.T., Yaksh, T.L., 2010. Effects of intrathecal ketorolac on human experimental pain. Anesthesiology 112, 1216–1224.
Fritsch, L.E., Kelly, C., Pickrell, A.M., 2023. The role of STING signaling in central nervous system infection and neuroinflammatory disease. Wires Mech Dis e1597.
Goldmann, T., Wieghofer, P., Müller, P.F., Wolf, Y., Varol, D., Yona, S., Brendecke, S.M., Kierdorf, K., Staszewski, O., Datta, M., Luedde, T., Heikenwalder, M., Jung, S., Prinz, M., 2013. A new type of microglia gene targeting shows TAK1 to be pivotal in CNS autoimmune inflammation. Nat. Neurosci. 16, 1618–1626.
Grosser, T., Woolf, C.J., FitzGerald, G.A., 2017. Time for nonaddictive relief of pain. Science 355, 1026–1027.
Gulen, M.F., Samson, N., Keller, A., Schwabenland, M., Liu, C., Glück, S., Thacker, V.V., Favre, L., Mangeat, B., Kroese, L.J., Krimpenfort, P., Prinz, M., Ablasser, A., 2023. cGAS-STING drives ageing-related inflammation and neurodegeneration. Nature 620, 374–380.
Hargreaves, K., Dubner, R., Brown, F., Flores, C., Joris, J., 1988. A new and sensitive method for measuring thermal nociception in cutaneous hyperalgesia. Pain 32, 77–88.
Hu, Y., Chen, Y., Liu, T., Zhu, C., Wan, L., Yao, W., 2023. The bidirectional roles of the cGAS-STING pathway in pain processing: Cellular and molecular mechanisms. Biomed. Pharmacother. 163, 114869.
Huang, L., Li, L., Lemos, H., Chandler, P.R., Pacholczyk, G., Baban, B., Barber, G.N., Hayakawa, Y., McGaha, T.L., Ravishankar, B., Munn, D.H., Mellor, A.L., 2013. Cutting edge: DNA sensing via the STING adaptor in myeloid dendritic cells induces potent tolerogenic responses. J. Immunol. 191, 3509–3513.
Ishikawa, H., Barber, G.N., 2008. STING is an endoplasmic reticulum adaptor that facilitates innate immune signalling. Nature 455, 674–678.
Ishikawa, H., Ma, Z., Barber, G.N., 2009. STING regulates intracellular DNA-mediated, type I interferon-dependent innate immunity. Nature 461, 788–792.
Jensen, T.S., Finnerup, N.B., 2014. Allodynia and hyperalgesia in neuropathic pain: clinical manifestations and mechanisms. Lancet Neurol. 13, 924–935.
Ji, R.R., Berta, T., Nedergaard, M., 2013. Glia and pain: is chronic pain a gliopathy? Pain 154 (Suppl 1), S10–S28.

Ji, R.R., Xu, Z.Z., Gao, Y.J., 2014. Emerging targets in neuroinflammation-driven chronic pain. Nat. Rev. Drug Discov. 13, 533–548.
Jiang, C.L., Son, L.X., Lu, C.L., You, Z.D., Wang, Y.X., Sun, L.Y., Cui, R.Y., Liu, X.Y., 2000. Analgesic effect of interferon-alpha via mu opioid receptor in the rat. Neurochem. Int. 36, 193–196.
Kaiser, T., Feng, G., 2019. Tmem119-EGFP and Tmem119-CreERT2 transgenic mice for labeling and manipulating microglia. eNeuro 6.
Keren-Shaul, H., Spinrad, A., Weiner, A., Matcovitch-Natan, O., Dvir-Szternfeld, R., Ulland, T.K., David, E., Baruch, K., Lara-Astaiso, D., Toth, B., Itzkovitz, S., Colonna, M., Schwartz, M., Amit, I., 2017. A unique microglia type associated with restricting development of alzheimer's disease. Cell 169, 1276–1290.e1217.
Kim, Y.S., Anderson, M., Park, K., Zheng, Q., Agarwal, A., Gong, C., Saijilafu, Y.L., He, S., LaVinka, P.C., Zhou, F., Bergles, D., Hanani, M., Guan, Y., Spray, D.C., Dong, X., 2016. Coupled activation of primary sensory neurons contributes to chronic pain. Neuron 91, 1085–1096.
Kim, D.S., Endo, A., Fang, F.G., Huang, K.C., Bao, X., Choi, H.W., Majumder, U., Shen, Y. Y., Mathieu, S., Zhu, X., Sanders, K., Noland, T., Hao, M.H., Chen, Y., Wang, J.Y., Yasui, S., TenDyke, K., Wu, J., Ingersoll, C., Loiacono, K.A., Hutz, J.E., Sarwar, N., 2021. E7766, a macrocycle-bridged stimulator of interferon genes (STING) agonist with potent pan-genotypic activity. ChemMedChem 16, 1740–1743.
Kohno, K., Shirasaka, R., Yoshihara, K., Mikuriya, S., Tanaka, K., Takanami, K., Inoue, K., Sakamoto, H., Ohkawa, Y., Masuda, T., Tsuda, M., 2022. A spinal microglia population involved in remitting and relapsing neuropathic pain. Science 376, 86–90.
Kong, X., Zuo, H., Huang, H.D., Zhang, Q., Chen, J., He, C., Hu, Y., 2023. STING as an emerging therapeutic target for drug discovery: Perspectives from the global patent landscape. J. Adv. Res. 44, 119–133.
Lacagnina, M.J., Watkins, L.R., Grace, P.M., 2018. Toll-like receptors and their role in persistent pain. Pharmacol. Ther. 184, 145–158.
Lee, S.H., Cho, P.S., Tonello, R., Lee, H.K., Jang, J.H., Park, G.Y., Hwang, S.W., Park, C. K., Jung, S.J., Berta, T., 2018. Peripheral serotonin receptor 2B and transient receptor potential channel 4 mediate pruritus to serotonergic antidepressants in mice. J. Allergy Clin. Immunol. 142, 1349–1352.e1316.
Li, Q., Barres, B.A., 2018. Microglia and macrophages in brain homeostasis and disease. Nat. Rev. Immunol. 18, 225–242.
Li, L., Ru, Q., Lu, Y., Fang, X., Chen, G., Saifullah, A.B., Yao, C., Tolias, K.F., 2023. Tiam1 coordinates synaptic structural and functional plasticity underpinning the pathophysiology of neuropathic pain. Neuron 111, 2038–2050.e2036.
Lin, C.Y., Guu, T.W., Lai, H.C., Peng, C.Y., Chiang, J.Y., Chen, H.T., Li, T.C., Yang, S.Y., Su, K.P., Chang, J.P., 2020. Somatic pain associated with initiation of interferon-alpha (IFN-α) plus ribavirin (RBV) therapy in chronic HCV patients: A prospective study. Brain Behav Immun Health 2, 100035.
Liu, C.C., Gao, Y.J., Luo, H., Berta, T., Xu, Z.Z., Ji, R.R., Tan, P.H., 2016. Interferon alpha inhibits spinal cord synaptic and nociceptive transmission via neuronal-glial interactions. Sci. Rep. 6, 34356.
Liu, S., Karaganis, S., Mo, R.F., Li, X.X., Wen, R.X., Song, X.J., 2020. IFNβ Treatment Inhibits Nerve Injury-induced Mechanical Allodynia and MAPK Signaling By Activating ISG15 in Mouse Spinal Cord. J. Pain 21, 836–847.
Liu, X., Tonello, R., Ling, Y., Gao, Y.J., Berta, T., 2019. Paclitaxel-activated astrocytes produce mechanical allodynia in mice by releasing tumor necrosis factor-α and stromal-derived cell factor 1. J. Neuroinflammation 16, 209.
Madisen, L., Zwingman, T.A., Sunkin, S.M., Oh, S.W., Zariwala, H.A., Gu, H., Ng, L.L., Palmiter, R.D., Hawrylycz, M.J., Jones, A.R., Lein, E.S., Zeng, H., 2010. A robust and high-throughput Cre reporting and characterization system for the whole mouse brain. Nat. Neurosci. 13, 133–140.
Mathur, V., Burai, R., Vest, R.T., Bonanno, L.N., Lehallier, B., Zardeneta, M.E., Mistry, K. N., Do, D., Marsh, S.E., Abud, E.M., Blurton-Jones, M., Li, L., Lashuel, H.A., Wyss-Coray, T., 2017. Activation of the STING-Dependent Type I Interferon Response Reduces Microglial Reactivity and Neuroinflammation. Neuron 96, 1290–1302. e1296.
McKelvey, R., Berta, T., Old, E., Ji, R.R., Fitzgerald, M., 2015. Neuropathic pain is constitutively suppressed in early life by anti-inflammatory neuroimmune regulation. J. Neurosci. 35, 457–466.
McLellan, M.A., Rosenthal, N.A., Pinto, A.R., 2017. Cre-loxP-mediated recombination: general principles and experimental considerations. Curr Protoc Mouse Biol 7, 1–12.
Meric-Bernstam, F., Sweis, R.F., Hodi, F.S., Messersmith, W.A., Andtbacka, R.H.I., Ingham, M., Lewis, N., Chen, X., Pelletier, M., Chen, X., Wu, J., McWhirter, S.M., Müller, T., Nair, N., Luke, J.J., 2022. Phase I dose-escalation trial of MIW815 (ADU-S100), an intratumoral STING agonist, in patients with advanced/metastatic solid tumors or lymphomas. Clin. Cancer Res. 28, 677–688.
Meric-Bernstam, F., Sweis, R.F., Kasper, S., Hamid, O., Bhatia, S., Dummer, R., Stradella, A., Long, G.V., Spreafico, A., Shimizu, T., Steeghs, N., Luke, J.J., McWhirter, S.M., Müller, T., Nair, N., Lewis, N., Chen, X., Bean, A., Kattenhorn, L., Pelletier, M., Sandhu, S., 2023. Combination of the STING agonist MIW815 (ADU-S100) and PD-1 inhibitor spartalizumab in advanced/metastatic solid tumors or lymphomas: an open-label, multicenter, phase Ib study. Clin. Cancer Res. 29, 110–121.
Motedayen Aval, L., Pease, J.E., Sharma, R., Pinato, D.J., 2020. Challenges and opportunities in the clinical development of STING agonists for cancer immunotherapy. J. Clin. Med. 9.
Olah, M., Patrick, E., Villani, A.C., Xu, J., White, C.C., Ryan, K.J., Piehowski, P., Kapasi, A., Nejad, P., Cimpean, M., Connor, S., Yung, C.J., Frangieh, M., McHenry, A., Elyaman, W., Petyuk, V., Schneider, J.A., Bennett, D.A., De Jager, P.L., Bradshaw, E.M., 2018. A transcriptomic atlas of aged human microglia. Nat. Commun. 9, 539.
Olah, M., Menon, V., Habib, N., Taga, M.F., Ma, Y., Yung, C.J., Cimpean, M., Khairallah, A., Coronas-Samano, G., Sankowski, R., Grün, D., Kroshilina, A.A., Dionne, D., Sarkis, R.A., Cosgrove, G.R., Helgager, J., Golden, J.A., Pennell, P.B., Prinz, M., Vonsattel, J.P.G., Teich, A.F., Schneider, J.A., Bennett, D.A., Regev, A., Elyaman, W., Bradshaw, E.M., De Jager, P.L., 2020. Single cell RNA sequencing of human microglia uncovers a subset associated with Alzheimer's disease. Nat. Commun. 11, 6129.
Ostenfeld, T., Krishen, A., Lai, R.Y., Bullman, J., Green, J., Anand, P., Scholz, J., Kelly, M., 2015. A randomized, placebo-controlled trial of the analgesic efficacy and safety of the p38 MAP kinase inhibitor, losmapimod, in patients with neuropathic pain from lumbosacral radiculopathy. Clin. J. Pain 31, 283–293.
Percie Du Sert, N., Ahluwalia, A., Alam, S., Avey, M.T., Baker, M., Browne, W.J., Clark, A., Cuthill, I.C., Dirnagl, U., Emerson, M., Garner, P., Holgate, S.T., Howells, D.W., Hurst, V., Karp, N.A., Lazic, S.E., Lidster, K., Maccallum, C.J., Macleod, M., Pearl, E.J., Petersen, O.H., Rawle, F., Reynolds, P., Rooney, K., Sena, E. S., Silberberg, S.D., Steckler, T., Würbel, H., 2020. Reporting animal research: Explanation and elaboration for the ARRIVE guidelines 2.0. PLoS Biol. 18, e3000411.
Posillico, C.K., Garcia-Hernandez, R.E., Tronson, N.C., 2021. Sex differences and similarities in the neuroimmune response to central administration of poly I:C. J. Neuroinflammation 18, 193.
Pujantell, M., Altfeld, M., 2022. Consequences of sex differences in Type I IFN responses for the regulation of antiviral immunity. Front. Immunol. 13, 986840.
Qin, Z.F., Hou, D.Y., Fang, Y.Q., Xiao, H.J., Wang, J., Li, K.C., 2012. Interferon-alpha enhances excitatory transmission in substantia gelatinosa neurons of rat spinal cord. Neuroimmunomodulation 19, 235–240.
Schmittgen, T.D., Livak, K.J., 2008. Analyzing real-time PCR data by the comparative C (T) method. Nat. Protoc. 3, 1101–1108.
Scholz, J., Woolf, C.J., 2007. The neuropathic pain triad: neurons, immune cells and glia. Nat. Neurosci. 10, 1361–1368.
Shih, A.Y., Damm-Ganamet, K.L., Mirzadegan, T., 2018. Dynamic structural differences between human and mouse STING lead to differing sensitivity to DMXAA. Biophys. J . 114, 32–39.
Sorge, R.E., Mapplebeck, J.C., Rosen, S., Beggs, S., Taves, S., Alexander, J.K., Martin, L. J., Austin, J.S., Sotocinal, S.G., Chen, D., Yang, M., Shi, X.Q., Huang, H., Pillon, N.J., Bilan, P.J., Tu, Y., Klip, A., Ji, R.R., Zhang, J., Salter, M.W., Mogil, J.S., 2015. Different immune cells mediate mechanical pain hypersensitivity in male and female mice. Nat. Neurosci. 18, 1081–1083.
Stokes, J.A., Corr, M., Yaksh, T.L., 2013. Spinal toll-like receptor signaling and nociceptive processing: regulatory balance between TIRAP and TRIF cascades mediated by TNF and IFNβ. Pain 154, 733–742.
Sun, J., Zhou, Y.Q., Xu, B.Y., Li, J.Y., Zhang, L.Q., Li, D.Y., Zhang, S., Wu, J.Y., Gao, S.J., Ye, D.W., Mei, W., 2022. STING/NF-κB/IL-6-Mediated Inflammation in Microglia Contributes to Spared Nerve Injury (SNI)-Induced Pain Initiation. J. Neuroimmune Pharmacol. 17, 453–469.
Talbot, K., Madden, V.J., Jones, S.L., Moseley, G.L., 2019. The sensory and affective components of pain: are they differentially modifiable dimensions or inseparable aspects of a unitary experience? A systematic review. Br. J. Anaesth. 123, e263–e272.
Tan, P.H., Gao, Y.J., Berta, T., Xu, Z.Z., Ji, R.R., 2012. Short small-interfering RNAs produce interferon-α-mediated analgesia. Br. J. Anaesth. 108, 662–669.
Tan, P.H., Ji, J., Yeh, C.C., Ji, R.R., 2021. Interferons in Pain and Infections: Emerging Roles in Neuro-Immune and Neuro-Glial Interactions. Front. Immunol. 12, 783725.
Tansley, S., Uttam, S., Ureña Guzmán, A., Yaqubi, M., Pacis, A., Parisien, M., Deamond, H., Wong, C., Rabau, O., Brown, N., Haglund, L., Ouellet, J., Santaguida, C., Ribeiro-Da-Silva, A., Tahmasebi, S., Prager-Khoutorsky, M., Ragoussis, J., Zhang, J., Salter, M.W., Diatchenko, L., Healy, L.M., Mogil, J.S., Khoutorsky, A., 2022. Single-cell RNA sequencing reveals time- and sex-specific responses of mouse spinal cord microglia to peripheral nerve injury and links ApoE to chronic pain. Nature. Communications 13.
Taves, S., Berta, T., Liu, D.L., Gan, S., Chen, G., Kim, Y.H., Van de Ven, T., Laufer, S., Ji, R.R., 2016. Spinal inhibition of p38 MAP kinase reduces inflammatory and neuropathic pain in male but not female mice: Sex-dependent microglial signaling in the spinal cord. Brain Behav. Immun. 55, 70–81.
Thomson, D.W., Poeckel, D., Zinn, N., Rau, C., Strohmer, K., Wagner, A.J., Graves, A.P., Perrin, J., Bantscheff, M., Duempelfeld, B., Kasparcova, V., Ramanjulu, J.M., Pesiridis, G.S., Muelbaier, M., Bergamini, G., 2019. Discovery of GSK8612, a Highly Selective and Potent TBK1 Inhibitor. ACS Med. Chem. Lett. 10, 780–785.
Tochitsky, I., Jo, S., Andrews, N., Kotoda, M., Doyle, B., Shim, J., Talbot, S., Roberson, D., Lee, J., Haste, L., Jordan, S.M., Levy, B.D., Bean, B.P., Woolf, C.J., 2021. Inhibition of inflammatory pain and cough by a novel charged sodium channel blocker. Br. J. Pharmacol. 178, 3905–3923.
Tonello, R., Xie, W., Lee, S.H., Wang, M., Liu, X., Strong, J.A., Zhang, J.M., Berta, T., 2020. Local Sympathectomy Promotes Anti-inflammatory Responses and Relief of Paclitaxel-induced Mechanical and Cold Allodynia in Mice. Anesthesiology 132, 1540–1553.
Udeochu, J.C., Amin, S., Huang, Y., Fan, L., Torres, E.R.S., Carling, G.K., Liu, B., McGurran, H., Coronas-Samano, G., Kauwe, G., Mousa, G.A., Wong, M.Y., Ye, P., Nagiri, R.K., Lo, I., Holtzman, J., Corona, C., Yarahmady, A., Gill, M.T., Raju, R.M., Mok, S.A., Gong, S., Luo, W., Zhao, M., Tracy, T.E., Ratan, R.R., Tsai, L.H., Sinha, S. C., Gan, L., 2023. Tau activation of microglial cGAS-IFN reduces MEF2C-mediated cognitive resilience. Nat. Neurosci. 26, 737–750.
Vanelderen, P., Van Zundert, J., Kozicz, T., Puylaert, M., De Vooght, P., Mestrum, R., Heylen, R., Roubos, E., Vissers, K., 2015. Effect of minocycline on lumbar radicular neuropathic pain: a randomized, placebo-controlled, double-blind clinical trial with amitriptyline as a comparator. Anesthesiology 122, 399–406.

Wang, K., Donnelly, C.R., Jiang, C., Liao, Y., Luo, X., Tao, X., Bang, S., McGinnis, A., Lee, M., Hilton, M.J., Ji, R.R., 2021. STING suppresses bone cancer pain via immune and neuronal modulation. Nat. Commun. 12, 4558.

Wang, X., Spandidos, A., Wang, H., Seed, B., 2012. PrimerBank: a PCR primer database for quantitative gene expression analysis, 2012 update. Nucleic Acids Res. 40, D1144–D1149.

Woller, S.A., Ocheltree, C., Wong, S.Y., Bui, A., Fujita, Y., Gonçalves Dos Santos, G., Yaksh, T.L., Corr, M., 2019. Neuraxial TNF and IFN-beta co-modulate persistent allodynia in arthritic mice. Brain Behav. Immun. 76, 151–158.

Wu, W., Zhang, X., Wang, S., Li, T., Hao, Q., Li, S., Yao, W., Sun, R., 2022. Pharmacological inhibition of the cGAS-STING signaling pathway suppresses microglial M1-polarization in the spinal cord and attenuates neuropathic pain. Neuropharmacology 217, 109206.

Yang, J., Ding, H., Shuai, B., Zhang, Y., Zhang, Y., 2022. Mechanism and effects of STING-IFN-I pathway on nociception: A narrative review. Front. Mol. Neurosci. 15, 1081288.

Younger, J., Mackey, S., 2009. Fibromyalgia symptoms are reduced by low-dose naltrexone: a pilot study. Pain Med. 10, 663–672.

Yu, X., Liu, H., Hamel, K.A., Morvan, M.G., Yu, S., Leff, J., Guan, Z., Braz, J.M., Basbaum, A.I., 2020. Dorsal root ganglion macrophages contribute to both the initiation and persistence of neuropathic pain. Nat. Commun. 11, 264.

Zhang, Y., Chen, K., Sloan, S.A., Bennett, M.L., Scholze, A.R., O'Keeffe, S., Phatnani, H.P., Guarnieri, P., Caneda, C., Ruderisch, N., Deng, S., Liddelow, S.A., Zhang, C., Daneman, R., Maniatis, T., Barres, B.A., Wu, J.Q., 2014. An RNA-sequencing transcriptome and splicing database of glia, neurons, and vascular cells of the cerebral cortex. J. Neurosci. 34, 11929–11947.

Zhang, X., Li, X., Wang, W., Zhang, Y., Gong, Z., Peng, Y., Wu, J., You, X., 2022. STING contributes to cancer-induced bone pain by promoting M1 Polarization of microglia in the medial prefrontal cortex. Cancers 14, 5188.

Zheng, Q., Xie, W., Lückemeyer, D.D., Lay, M., Wang, X.W., Dong, X., Limjunyawong, N., Ye, Y., Zhou, F.Q., Strong, J.A., Zhang, J.M., Dong, X., 2022. Synchronized cluster firing, a distinct form of sensory neuron activation, drives spontaneous pain. Neuron 110, 209–220.e206.